In summary, the cytoplasmic and nuclear expression of S100A4 is stronger in ovarian carcinomas than in benign or borderline tumors, and nuclear expression of S100A4 could be an indicator for poor prognosis in ovarian carcinoma patients. In addition, ovarian carcinoma cells express S100A4 at the mRNA and protein levels and secrete S100A4, which might in turn work for its own upregulation as well as its nuclear translocation, along with an enhancement of invasiveness *in vitro*. Thus, S100A4 might be an important autocrine/paracrine factor involved in the aggressive characteristics of ovarian carcinoma cells, and could be a molecular target in the treatment of ovarian carcinoma. Development of a novel therapy targeted to the S100A4-RhoA pathway is needed to improve the survival of ovarian carcinoma patients.

## Acknowledgments

This work was supported in part by Grants-in-Aid for Scientific Research from the Ministry of Education, Science and Culture (No. 15390502, No. 16790947), Japan.

## References

1 Murdoch WJ. Ovarian surface epithelium, ovulation and carcinogenesis. *Biol Rev Camb Philos Soc* 1996; **71**: 529–43.
2 Mandai M, Konishi I, Komatsu T *et al.* Mutation of the *nm23* gene, loss of heterozygosity at the *nm23* locus and K-ras mutation in ovarian carcinoma: correlation with tumour progression and *nm23* gene expression. *Br J Cancer* 1995; **72**: 691–5.
3 Imai T, Horiuchi A, Wang C *et al.* Hypoxia attenuates the expression of E-cadherin via up-regulation of SNAIL in ovarian carcinoma cells. *Am J Pathol* 2003; **163**: 1437–47.
4 Bernstein LR, Liotta LA. Molecular mediators of interactions with extracellular matrix components in metastasis and angiogenesis. *Curr Opin Oncol* 1994; **6**: 106–13.
5 Schmalfeldt B, Prechtel D, Harting K *et al.* Increased expression of matrix metalloproteinases (MMP)-2, MMP-9, and the urokinase-type plasminogen activator is associated with progression from benign to advanced ovarian cancer. *Clin Cancer Res* 2001; **7**: 2396–404.
6 Baserga R. Oncogenes and the strategy of growth factors. *Cell* 1994; **79**: 927–30.
7 Yamamoto S, Konishi I, Mandai M *et al.* Expression of vascular endothelial growth factor (VEGF) in epithelial ovarian neoplasms: correlation with clinicopathology and patient survival, and analysis of serum VEGF levels. *Br J Cancer* 1997; **76**: 1221–7.
8 Horiuchi A, Imai T, Shimizu M *et al.* Hypoxia-induced changes in the expression of VEGF, HIF-1 alpha and cell cycle-related molecules in ovarian cancer cells. *Anticancer Res* 2002; **22**: 2697–702.
9 Horiuchi A, Imai T, Wang C *et al.* Up-regulation of small GTPases, RhoA and RhoC, is associated with tumor progression in ovarian carcinoma. *Laboratory Invest* 2003; **83**: 861–70.
10 Donato R. S100: a multigenic family of calcium-modulated proteins of the EF-hand type with intracellular and extracellular functional roles. *Int J Biochem Cell Biol* 2001; **33**: 637–68.
11 Selinfreund RH, Barger SW, Welsh MJ, Van Eldik LJ. Antisense inhibition of glial S100 beta production results in alterations in cell morphology, cytoskeletal organization, and cell proliferation. *J Cell Biol* 1990; **111**: 2021–8.
12 Davies BR, Davies MP, Gibbs FE, Barraclough R, Rudland PS. Induction of the metastatic phenotype by transfection of a benign rat mammary epithelial cell line with the gene for p9Ka, a rat calcium-binding protein, but not with the oncogene EJ-ras-1. *Oncogene* 1993; **8**: 999–1008.
13 Davies MP, Rudland PS, Robertson L, Parry EW, Jolicoeur P, Barraclough R. Expression of the calcium-binding protein S100A4 (p9Ka) in MMTV-neu transgenic mice induces metastasis of mammary tumors. *Oncogene* 1996; **13**: 1631–7.
14 Parker C, Whittaker PA, Usmani BA, Lakshmi MS, Sherbet GV. Induction of 18A2/mts1 gene expression and its effects on metastasis and cell cycle control. *DNA Cell Biol* 1994; **13**: 1021–8.
15 Ilg EC, Schafer BW, Heizmann CW. Expression pattern of S100 calcium-binding proteins in human tumors. *Int J Cancer* 1996; **68**: 325–2.
16 Novitskaya V, Grigorian M, Kriajevska M *et al.* Oligomeric forms of the metastasis-related Mts1 (S100A4): protein stimulate neuronal differentiation in cultures of rat hippocampal neurons. *J Biol Chem* 2000; **275**: 41278–86.
17 Semov A, Moreno MJ, Onichtchenko A *et al.* Metastasis-associated protein S100A4 induces angiogenesis through interaction with annexin II and accelerated plasmin formation. *J Biol Chem* 2005; **280**: 20833–41.
18 Mueller A, Bachi T, Hochli M, Schafer BW, Heizmann CW. Subcellular distribution of S100 proteins in tumor cells and their relocation in response to calcium activation. *Histochem Cell Biol* 1999; **111**: 453–9.
19 Silverberg SG. Histopathologic grading of ovarian carcinoma: a review and proposal. *Int J Gynecol Pathol* 2000; **19**: 7–15.
20 Scully RE, Young RH, Clement PB. Surface epithelial-stromal tumors and serous tumors. In: Rosai J, Sobin LH, eds. *Atlas of Tumor Pathology. Tumors of the Ovary, Maldeveloped Gonads, Fallopian Tube, and Broad Ligamant.* Third series, Fascicle 23. Washington DC: Armed Forces Institute of Pathology, 1998.
21 Davies BR, O'Donnell M, Durkan GC *et al.* Expression of S100A4 protein is associated with metastasis and reduced survival in human bladder cancer. *J Pathol* 2002; **196**: 292–9.
22 Pedersen KB, Nesland JM, Fodstad O, Maelandsmo GM. Expression of S100A4, E-cadherin, alpha- and beta-catenin in breast cancer biopsies. *Br J Cancer* 2002; **87**: 1281–6.
23 Tsuruo T, Hamilton TC, Louie KG, Behrens BC, Young RC, Ozols RF. Collateral susceptibility of adriamycin-, melphalan- and cisplatin-resistant human ovarian tumor cells to bleomycin. *Jpn J Cancer Res* 1986; **77**: 941–5.
24 Chomczynski P, Sacchi N. Single-step method of RNA isolation by acid guanidinium thiocyanate-phenol-chloroform extraction. *Anal Biochem* 1987; **162**: 156–9.
25 Albini A, Iwamoto Y, Kleinman HK *et al.* A rapid *in vitro* assay for quantitating the invasive potential of tumor cells. *Cancer Res* 1987; **47**: 3239–45.
26 Ito T, Williams JD, Fraser D, Phillips AO. Hyaluronan attenuates transforming growth factor-beta1-mediated signaling in renal proximal tubular epithelial cells. *Am J Pathol* 2004; **164**: 1979–88.
27 Bjornland K, Winberg JO, Odegaard OT *et al.* S100A4 involvement in metastasis: deregulation of matrix metalloproteinases and tissue inhibitors of matrix metalloproteinases in osteosarcoma cells transfected with an anti-S100A4 ribozyme. *Cancer Res* 1999; **59**: 4702–8.
28 Sato N, Fukushima N, Maitra A *et al.* Gene expression profiling identifies genes associated with invasive intraductal papillary mucinous neoplasms of the pancreas. *Am J Pathol* 2004; **164**: 903–14.
29 Rudland PS, Platt-Higgins A, Renshaw C *et al.* Prognostic significance of the metastasis-inducing protein S100A4 (p9Ka) in human breast cancer. *Cancer Res* 2000; **60**: 1595–603.
30 Hsieh HL, Schafer BW, Weigle B, Heizmann CW. S100 protein translocation in response to extracellular S100 is mediated by receptor for advanced glycation endproducts in human endothelial cells. *Biochem Biophys Res Commun* 2004; **316**: 949–59.
31 Sakaguchi M, Miyazaki M, Inoue Y *et al.* Relationship between contact inhibition and intranuclear S100C of normal human fibroblasts. *J Cell Biol* 2000; **149**: 1193–206.
32 Davey GE, Murmann P, Heizmann CW. Intracellular $Ca^{2+}$ and $Zn^{2+}$ levels regulate the alternative cell density-dependent secretion of S100B in human glioblastoma cells. *Biol Chem* 2001; **276**: 30819–26.
33 Flatmark K, Pedersen KB, Nesland JM *et al.* Nuclear localization of the metastasis-related protein S100A4 correlates with tumour stage in colorectal cancer. *J Pathol* 2003; **200**: 589–95.
34 Mandinova A, Atar D, Schafer BW, Spiess M, Aebi U, Heizmann CW. Distinct subcellular localization of calcium binding S100 proteins in human smooth muscle cells and their relocation in response to rises in intracellular calcium. *J Cell Sci* 1998; **111**: 2043–54.
35 Jenkinson SR, Barraclough R, West CR, Rudland PS. S100A4 regulates cell motility and invasion in an *in vitro* model for breast cancer metastasis. *Br J Cancer* 2004; **90**: 253–62.
36 Schmidt-Hansen B, Ornas D, Grigorian M *et al.* Extracellular S100A4 (mts1) stimulates invasive growth of mouse endothelial cells and modulates MMP-13 matrix metalloproteinase activity. *Oncogene* 2004; **23**: 5487–95.
37 Mathisen B, Lindstad RI, Hansen J *et al.* S100A4 regulates membrane induced activation of matrix metalloproteinase-2 in osteosarcoma cells. *Clin Exp Metastasis* 2003; **20**: 701–11.
38 Ambartsumian N, Klingelhofer J, Grigorian M *et al.* The metastasis-associated Mts1 (S100A4): protein could act as an angiogenic factor. *Oncogene* 2001; **20**: 4685–95.

British Journal of Cancer (2005) 92, 1737–1745

www.bjcancer.com

# Clinical significance of heparin-binding epidermal growth factor-like growth factor in peritoneal fluid of ovarian cancer

**H Yagi[1], S Miyamoto*[,1], Y Tanaka[1], K Sonoda[1], H Kobayashi[1], T Kishikawa[2], R Iwamoto[3], E Mekada[3] and H Nakano[1]**

*[1]Department of Obstetrics and Gynecology, Graduate School of Medical Sciences, Kyushu University, 3-1-1 Maidashi, Higashi-ku, Fukuoka 812-8582, Japan; [2]Department of Obstetrics and Gynecology, Saiseikai Fukuoka General Hospital, 1-3-46 Tenjin, Chuo-ku, Fukuoka 810-0001, Japan; [3]Department of Cell Biology, Research Institute for Microbial Diseases, Osaka University, 3-1 Yamadaoka, Suita, Osaka 565-0871, Japan*

Epidermal growth factor receptor (EGFR) has been implicated in tumour growth and extension of ovarian cancer. Peritoneal fluid in ovarian cancer patients contains various growth factors that can promote tumour growth and extension. In order to investigate the clinical significance of EGFR ligands as activating factors of ovarian cancer, we examined the cell proliferation-promoting activity and the level of EGFR ligands in peritoneal fluid obtained from 99 patients. Proliferation-promoting activity in peritoneal fluid from 63 ovarian cancer patients (OVCA) was much higher than peritoneal fluid from 18 ovarian cyst patients (OVC) and 18 normal ovary patients (NO), and the activity was suppressed only by antibodies against EGFR or heparin-binding epidermal growth factor (HB-EGF). A large difference was observed in the level of EGFR ligands between HB-EGF and TGF-$\alpha$ or amphiregulin. The concentration of HB-EGF in OVCA significantly increased compared to that in OVC or NO ($P<0.01$). No significant difference in the concentration of TGF-$\alpha$ and amphiregulin was found between the OVCA and NO or OVC groups. In peritoneal fluid, HB-EGF is sufficiently elevated to activate cancer cells even at an early stage of OVCA. These results suggested that HB-EGF in peritoneal fluid might play a key role in cell survival and in the proliferation of OVCA.
*British Journal of Cancer* (2005) **92,** 1737–1745. doi:10.1038/sj.bjc.6602536 www.bjcancer.com
Published online 12 April 2005


**Keywords:** ovarian cancer; HB-EGF; EGFR; peritoneal fluid

Ovarian cancer (OVCA) is the most frequent cause of cancer death among all gynaecologic cancers, and in the last 30 years current therapies have not improved cure rates (Penson *et al*, 1998). The high mortality is caused predominantly by the occult progression of the tumour into the peritoneal cavity with an initial diagnosis usually being made at an advanced stage. Tumour growth is characterised by local extension into the peritoneal cavity following the circulatory pathway of the peritoneal fluid produced by peritoneal epithelium and cancer cells. Accumulated evidence from many studies reveals that ascites from OVCA patients is a rich source of growth factor activity for OVCA cells, termed ovarian cancer activating factors (OCAFs) (Mills *et al*, 1998). The dissemination of cancer cells activated by OCAFs result in an exaggerated increase in peritoneal fluid, which in turn leads to tumour extension of OVCA.

To identify OCAFs of OVCA, various peptide growth factors and cytokines have been detected in the malignant effusions of OVCA patients (Westermann *et al*, 1997). However, the growth-promoting properties of malignant effusions *in vivo* and *in vitro* have been shown to be independent of these peptide growth factors (Westermann *et al*, 1997). Recent biochemical analysis has revealed that one possible OCAF candidate is lysophophatidic acid (LPA) (Xu *et al*, 1995; Westermann *et al*, 1998; Xiao *et al*, 2001). Lysophophatidic acid is a simple phospholipid with numerous cellular effects including growth promotion, cell cycle progression and cytoskeletal organisation (Mills and Moolenaar, 2003). However, LPA may not be the sole mediator present in ascites because the proliferation of cancer cells was lower than that induced by ascites from OVCA patients, even at optimal LPA concentrations (Xu *et al*, 1995).

Impairment of the epidermal growth factor (EGF) system has been implicated in the pathogenesis of different types of carcinomas (Salomon *et al*, 1995; Normanno *et al*, 2003). As described in the literature (Salomon *et al*, 1995; Normanno *et al*, 2003), EGF receptor (EGFR) overexpression occurs in 35–70% of all primary OVCAs and the overexpression of ErbB2 is correlated to clinical outcome. Whereas the frequency of ErbB2 overexpression is low, the frequencies of ErbB3 and ErbB4 expressions are high in OVCA. Univariate and multivariate statistical analyses have confirmed that EGFR overexpression is significantly associated with a high risk of progression in OVCA patients (Scambia *et al*, 1992). Seven ligands have been described for EGFR: EGF, transforming growth factor-$\alpha$ (TGF-$\alpha$). heparin-binding-EGF like growth factor (HB-EGF), amphiregulin (AR), betacellulin, epiregulin, and epigen (Fischer *et al*, 2003). All are synthesised as membrane-spanning precursor molecules that have to be proteolytically processed to become fully active (Fischer *et al*, 2003). A relatively high frequency of TGF-$\alpha$ and AR has been described in ovarian carcinomas, although staining in tumours varied from weak to

*Correspondence: Dr S Miyamoto; E-mail: smiya@med.kyushu-u.ac.jp
Received 4 October 2004; revised 17 February 2005; accepted 28 February 2005; published online 12 April 2005

strong (Morishige *et al*, 1991; D'Antonio *et al*, 2002). Ovarian cancer cells are sensitive to diphtheria toxin, indicating the expression of proHB-EGF (Morimoto *et al*, 1991). We reported that HB-EGF is involved in EGFR signal transactivation induced by LPA in OVCA cell lines, and that the soluble form of HB-EGF is attributable to tumour growth on xenografted mice using OVCA cell lines (Miyamoto *et al*, 2004). On the basis of these results, it is suggested that EGFR plays a pivotal role in the acceleration and progression of ovarian caner through EGFR ligands including TGF-$\alpha$, HB-EGF, and AR.

The concentration of EGFR ligands was examined to determine their role as tumour-promoting factors in the peritoneal fluid of OVCA patients. Peritoneal fluid of OVCA patients was also examined for proliferation-promoting and cell survival activities in OVCA cells in the absence or presence of specific inhibitory antibodies against EGFR and EGFR ligands.

## MATERIALS AND METHODS

### Patients and peritoneal fluids

All of the 99 patients in this study underwent surgery between 1994 and August 2003 at the Department of Obstetrics and Gynecology, Kyushu University Hospital. Peritoneal fluids were obtained from 99 women, who gave signed informed consent (Table 1). In all, 18 cases with normal ovaries had surgical treatment due to uterine myomas or benign gynaecologic disorders. In six cases with marked ascites and multiple disseminating sites in the peritoneum, peritoneal fluids were obtained twice, once before chemotherapy and once after three courses of chemotherapy, under a presurgical state. Peritoneal fluid supernatants were collected immediately after centrifugation (3000 g $\times$ 15 min), and stored at $-80^{\circ}$C until use.

### Reagents

Recombinant human HB-EGF and synthetic LPA were purchased from R&D Systems Inc. (Minneapolis, MN, USA) and from Avanti Polar Lipids, Inc. (Alabaster, AL, USA), respectively. [$^3$H]thymidine (6.7 Ci mmol$^{-1}$) was obtained from New England Nuclear (Lachine, Quebec, Canada). Mouse anti-human EGF receptor neutralising antibody and goat anti-human HB-EGF neutralising antibody was obtained from Upstate Inc. (Lake Placid, NY, USA) and R&D Systems Inc. (Minneapolis, MN, USA), respectively. Goat anti-human TGF-$\alpha$ neutralising antibody, mouse anti-human AR neutralising antibody, mouse anti-human EGF neutralising antibody, goat anti-human epiregulin neutralising antibody and goat anti-human betacellulin neutralising antibody were also purchased from GT (Minneapolis, MN, USA). The manufacturer's instructions detail that at least 5 ng ml$^{-1}$ of EGFR and EGFR ligands (EGF, TGF-$\alpha$, HB-EGF, AR, betacellulin and epiregulin) can be neutralized in the use of 10 $\mu$g ml$^{-1}$ of these antibodies, respectively.

**Table 1** Clinical data for patients

| Variable | No. of patients | Age (years) (mean $\pm$ s.d.) | Histological types: Serous | Histological types: Others |
|---|---|---|---|---|
| Normal ovary | 18 | 55.5 $\pm$ 17.8 | | |
| Ovarian cyst | 18 | 54.6 $\pm$ 19.7 | 10 | 8 |
| Ovarian cancer, stage Ia | 10 | 57.2 $\pm$ 14.3 | 7 | 3 |
| Ovarian cancer, stage Ic–II | 13 | 55.8 $\pm$ 10.6 | 8 | 5 |
| Ovarian cancer, stage III–IV | 30 | 59.3 $\pm$ 16.2 | 22 | 8 |
| Ovarian cancer, recurrence | 10 | 58.2 $\pm$ 11.2 | 7 | 3 |

Polyclonal rabbit anti-EGFR and anti-ErbB-4 antibodies were obtained from Santa Cruz Biotechnology (Santa Cruz, CA, USA) and Upstate Biotechnology Inc. (Lake Placid, NY, USA), respectively. Peroxidase-conjugated goat anti-rabbit IgG was purchased from Zymed (San Francisco, CA, USA).

### Immunoblot

Cells were rinsed in phosphate-buffered saline (PBS) and then lysed in RIPA buffer (1% Triton X-100, 1% sodium deoxycholate, 0.1% SDS, 150 mM NaCl, 50 mM Tris (pH 8.0), 0.2 unist ml$^{-1}$ aprotinin, 2 $\mu$g ml$^{-1}$ leupeptin, 1 $\mu$g ml$^{-1}$ pepstatin A, 2 mM phenylmethylsulphonyl fluoride). In all, 50 $\mu$g of extracts wsa then subjected to SDS–polyacrylamide gel electrophoresis (SDS–PAGE) and immunoblotting analysis (Miyamoto *et al*, 2004).

### Cell proliferation-promoting assay mediated by factors in peritoneal fluid

SKOV3 cells, derived from OVCA, were maintained in RPMI-1640 (Nacalai Tesque Co. Ltd., Kyoto, Japan) supplemented with 10% (v v$^{-1}$) fetal bovine serum (FBS). To remove extracellular matrix components, cells were detached with trypsin-EDTA, then allowed to recover for 30 min in RPMI-1640 with 10% FBS. After rinsing with serum-free medium, cells were incubated with serum-free medium at 37°C for 30 min. Cells ($1 \times 10^4$) were seeded on poly-lysine-coated dishes, and samples incubated with serum-free RPMI-1640 at 37°C for 1 h to assure the complete adherence of cells to the poly-lysine-coated dishes. To assess cell proliferative activity, cells were incubated in 200 $\mu$l of RPMI-1640 plus 90% of each human peritoneal fluid at 37°C for 24 h; then WST-1 assay (Dojin Laboratory, Kumamoto, Japan) was performed according to the manufacturer's instructions. Further, to reconfirm the potential of the DNA polymerisation induced by peritoneal fluids, [$^3$H]thymidine incorporation was examined in SKOV 3 cells, using 10% human peritoneal fluid. The cells were treated in the same manner as the WST-1 assay, and the medium was then replaced with RPMI-1640 plus 10% of each human peritoneal fluid for an additional 24 h in the absence or presence of inhibitory antibodies against EGFR, HB-EGF, TGF-$\alpha$, amphiregulin, epiregulin, betacellulin, and EGF, or with RPMI-1640 plus 10% peritoneal fluid from patients with a normal ovary (NO) in the absence or presence of various concentrations of LPA or HB-EGF. Peritoneal fluids from 30 patients with OVCA (five cases at stage Ia, five at Ic-II, 15 at III–IV, and five of recurrence) were available for the experiment using inhibitory antibodies. [$^3$H]thymidine (1 $\mu$Ci well$^{-1}$) was then added to the cell culture. After 4 h of labelling with [$^3$H]thymidine, cells were washed with PBS, lysed with NaOH and treated with TCA. After adding scintillation fluid, [$^3$H]thymidine uptake was measured in a $\beta$-scintillation counter. Each experiment was conducted in triplicate. The mean value was considered as the representative value for each experiment. The WST-1 assay and the [$^3$H]thymidine incorporation were also examined in other OVCA cell lines including RMG-1 and OVMG1 cells in 10 cases with a NO and in 20 cases with OVCA.

### Inhibition of cell apoptotic assay mediated by factors in peritoneal fluid

The OVCA cell lines ($1 \times 10^5$) of SKOV3, RMG-1, and OVMG1 were treated in the same manner as in the WST-1 assay. Thereafter, this medium was replaced with the RPMI-1640 plus 10% of each human peritoneal fluid for an additional 24 h in the absence or presence of inhibitory antibodies against HB-EGF. Cells were harvested, pooled, and then fixed with 4% paraformaldehyde and 70% ethanol. After further washing in PBS, cells were incubated with TdT reaction reagent for 1 h at 37°C, according to the manufacturer's recommended protocol (MEBSTAIN Apoptosis Kit

Direct, MBL, Co., Ltd, Japan). TUNEL-positive cells were quantified as apoptotic cells by flow cytometric analysis (Becton Dickinson, FACScan, 01-20126-xx, USA).

### Binding assay for HB-EGF

The binding of $^{125}$I-diphtheria toxin (DT) to HB-EGF was measured as described previously (Iwamoto *et al*, 1994). Briefly, 1 ml of peritoneal fluid was incubated with heparin-sepharose CL-6B for 5 h at 4°C. The gel was washed three times with PBS and incubated with $^{125}$I-DT in the presence or absence of excess unlabelled DT for 12 h at 4°C. It was then washed three times with PBS and three times with high-salt PBS. The radioactivity bound to the gel was counted with a gamma counter, and the specific binding of $^{125}$I-DT to the HB-EGF molecule was calculated by subtracting the radioactivity of the sample in the presence of unlabelled DT from that of the sample in the absence of unlabelled DT. The amount of HB-EGF was estimated by the standard curve obtained using recombinant human HB-EGF. All experiments were conducted in triplicate and the mean HB-EGF value was regarded as the representative value of HB-EGF in each case.

### Immunoassay for human TGF-α and AR

Concentrations of TGF-α and AR in peritoneal fluid were determined with a commercially available ELISA (Quantikine Kit, R&D Systems Inc. and ELISA Development Kit, GT, Minneapolis, MN, USA) in accordance with the manufacturer's instructions. Samples were analysed in triplicate. Levels of TGF-α and AR were calculated from the linear areas of the standard curves obtained using Multiskan MS, version 8.0 (Labsystems, Helsinki, Finland), respectively. The mean value was used as the representative value. The lower limits for detection of TGF-α and AR were 5 and 10 pg ml$^{-1}$, respectively. When the amount was less than the detection limit, the TGF-α or AR value was recorded as 5 or 10 pg ml$^{-1}$, respectively.

### Statistical analysis

The statistical significance was assessed using the Mann–Whitney test and a *P*-value less than 0.05 was considered statistically significant.

## RESULTS

To investigate the expression of EGFR and ErbB-4 in the OVCA cell lines of SKOV3, RMG-1, and OVMG1, each protein expression was examined using immunoblotting analysis. The expression of EGFR in RMG-1 cells increased remarkably compared to those in SKOV3 or OVMG1 cells. There was little difference in the expression of ErbB4 among these three lines of OVCA cells (Figure 1A).

To assess the cell proliferative property mediated by factors in peritoneal fluid, cell proliferation of SKOV3 cells was examined using the WST-1 assay after incubation with peritoneal fluid. WST-1 assay demonstrated that the value in patients with OVCA significantly increased compared to that in patients with a NO or ovarian cyst (OVC) (Figure 1B and Table 2). To address whether peritoneal fluid from OVCA patients actually stimulates cancer cell proliferation, the proliferation of SKOV3 cells was examined by [$^3$H]thymidine incorporation into DNA. In the absence of the patient's peritoneal fluid, SKOV3 cells showed [$^3$H]thymidine incorporation at a minimum value (5800 ± 1200 cpm). Addition of peritoneal fluid resulted in increased DNA synthesis in all cases, but peritoneal fluid from OVCA patients enhanced DNA synthesis much highly than that from NO and OVC (each $P<0.01$) (Figure 1C and Table 2). In the WST-1 assay, the absorbances of the 10 cases with a NO and the 20 cases with OVCA were 0.31 ± 0.12 and 0.62 ± 0.23 (mean ± standard deviation) (RMG-1 cells), and 0.30 ± 0.13 and 0.69 ± 0.23 (OVMG1 cells), respectively. In RMG-1 and OVMG1 cells, the proliferative activity in peritoneal fluid of OVCA patients was significantly enhanced, compared with that in NO (both $P<0.01$). In [$^3$H]thymidine incorporation, the values in the 10 cases with a NO and the 20 cases with OVCA were 5823 ± 1066 c.p.m. (count per minute) and 9241 ± 1553 c.p.m (mean ± standard deviation) (RMG-1 cells), and 6903 ± 1134 c.p.m. and 12572 ± 1951 c.p.m. (OVMG1 cells), respectively. In RMG-1 and OVMG1 cells, the DNA polymerisation property mediated by peritoneal fluid in OVCA was also significantly elevated, compared with that in NO (both $P<0.01$). These results indicate that peritoneal fluid in patients with OVCA possesses a significant cell proliferative property.

To examine which EGFR ligands contribute to SKOV3 cell proliferation in a patient's peritoneal fluid, the effects of peritoneal fluid on SKOV3 cell DNA synthesis were measured in the absence or presence of an inhibitory antibody against EGFR or each EGFR ligand. [$^3$H]thymidine incorporation was significantly reduced in the presence of anti-EGFR or anti-HB-EGF neutralising antibody, while neutralising antibodies against TGF-α, AR, epiregulin, betacellulin, and EGF had no effect on [$^3$H]thymidine incorporation in SKOV3 cells (Figure 1D). The contribution of epigen was not determined, as no antibodies against epigen are available. In the presence of inhibitory antibodies against HB-EGF or EGFR, the values of [$^3$H]thymidine incorporation were 7301 ± 1093 and 7308 ± 1120 c.p.m (RMG-1 cells), and 9513 ± 1510 and 9160 ± 1296 c.p.m. (OVMG1 cells), respectively. [$^3$H]thymidine incorporation was also significantly reduced in the presence of anti-EGFR or anti-HB-EGF neutralising antibodies using RMG-1 or OVMG1 cells.

To evaluate the role of HB-EGF in cell survival in peritoneal fluid, apoptotic cells were analysed using the FACScan after staining cells by TUNEL methods in 10% human peritoneal fluid with an absence or presence of an inhibitory antibody against HB-EGF. Significant apoptotic cells in RMG-1 and OVMG1 cells were not observed even under serum-free conditions. In SKOV3 cells, 25.1 ± 1.4% (mean ± standard deviation) were detected as TUNEL-positive under serum-free conditions (Figure 2C). In a patient with a NO, there was no difference in the percentage of apoptotic cells between an absence or presence of peritoneal fluid, or between an absence or presence of the inhibitory antibody plus peritoneal fluid (Figure 2A). In a patient with OVCA, the percentage of apoptotic cells incubated with peritoneal fluid markedly decreased, compared to that incubated without peritoneal fluid (Figure 2B). As well, peritoneal fluid plus the inhibitory antibody against HB-EGF blocked any decrease of apoptotic cells (Figure 2B and C). In the 10 cases with a NO or the 20 cases with OVCA, the percentages of apoptotic cells were 24.6 ± 4.6 or 3.3 ± 2.2%, respectively, after incubation with peritoneal fluid (Figure 2C). In peritoneal fluid from OVCA patients in the presence of the inhibitory antibody against HB-EGF, the percentage of apoptotic cells significantly increased at 18.2 ± 5.2%, compared with that in the absence of the inhibitory antibody ($P<0.01$) (Figure 2C). These results suggest that HB-EGF in the peritoneal fluid of OVCA patients may contribute to cell survival in OVCA cells.

The present study suggests that HB-EGF levels may increase in peritoneal fluid from OVCA patients, and that HB-EGF is one of the factors in peritoneal fluid from OVCA patients that promotes tumour growth. Thus, HB-EGF, in addition to LPA, should be included as a member of OCAFs. To compare HB-EGF with LPA for proliferation-promoting activity, SKOV3 cells were cultured either with HB-EGF or LPA in a culture medium containing peritoneal fluid of NO patients. Although the concentration of LPA in the peritoneal fluid of OVCA patients

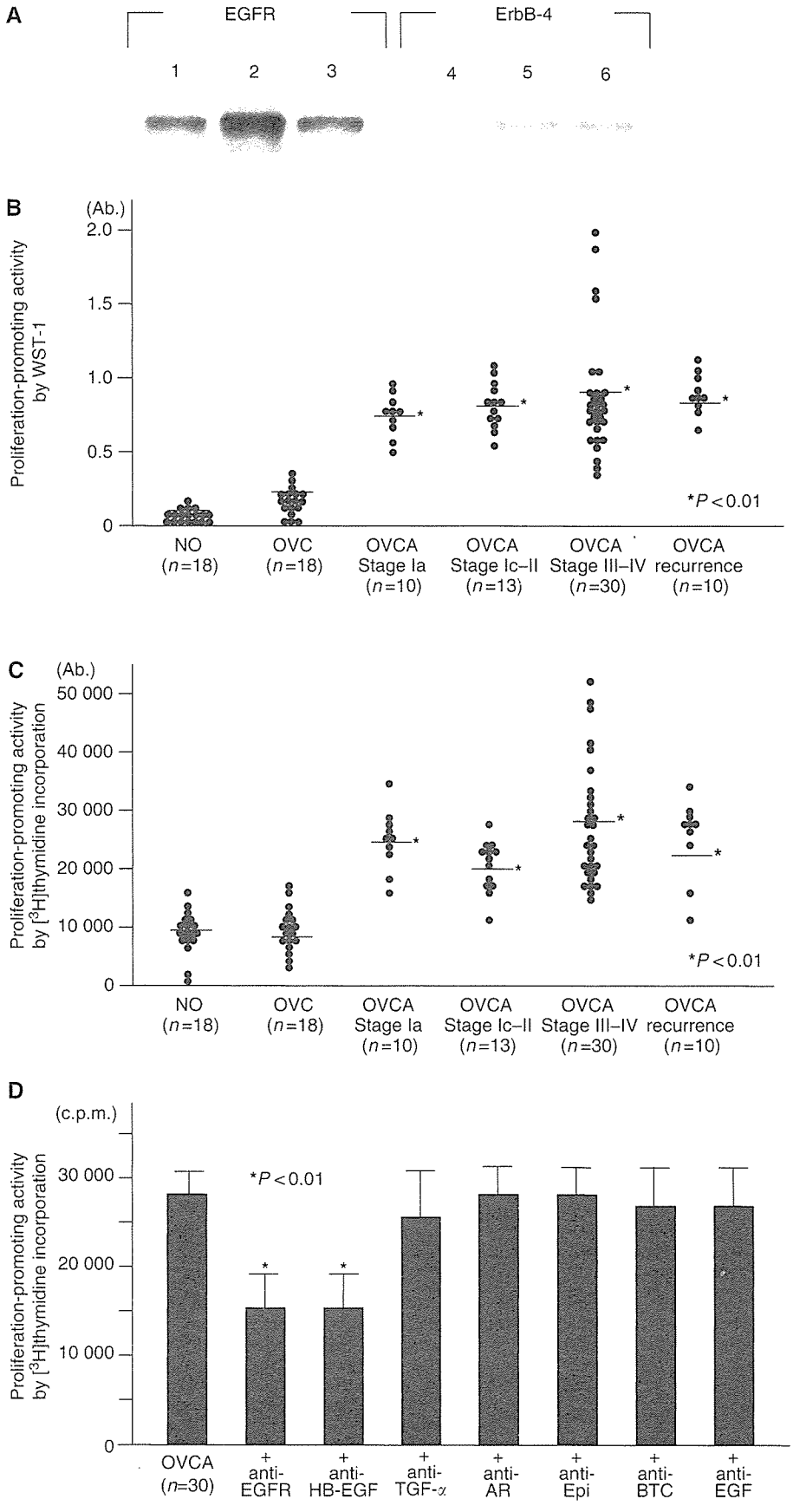

is reportedly from 10 to 20 $\mu$M (Xu *et al*, 1995; Westermann *et al*, 1998; Xiao *et al*, 2001), LPA (0–50 $\mu$M) did not show any growth-promoting effect in the present cell system (Figure 3A). In contrast, HB-EGF enhanced SKOV3 cell proliferation in a dose-dependent manner (Figure 3B), even at concentrations of 1–10 ng ml$^{-1}$, which are comparable to the levels of HB-EGF in peritoneal fluid of OVCA patients. These results indicate that HB-EGF induced significant cell proliferation, even in the presence of a concentration of 1 ng ml$^{-1}$.

To gain an insight into the role of EGFR ligands in peritoneal fluid of OVCA patients, the concentrations of HB-EGF, TGF-$\alpha$, and AR were determined in the peritoneal fluid of patients with a NO , OVC, and OVCA. Heparin-binding epidermal growth factor levels were significantly enhanced in all stages in OVCA patients compared with levels in NO and OVC patients ($P<0.01$) (Figure 4A and Table 2). Transforming growth factor-$\alpha$ levels were quite low (less than 40 pg ml$^{-1}$) in all cases, and 46 out of 99 cases (four cases of NO, six cases of OVC, 30 cases of OVCA, and six cases of recurrence of OVCA) showed levels lower than the detection limit (5 pg ml$^{-1}$). Amphiregulin levels were scattered among the cases, but were less than 1000 pg ml$^{-1}$ except in three OVCA cases. No significant differences were found in TGF-$\alpha$ and AR levels among the patients with NO, OVC, and OVCA (Figure 4B, C and Table 2). In addition to the significant increase of HB-EGF levels in OVCA patients, the concentration of HB-EGF in the peritoneal fluid of OVCA patients was much higher than those of TGF-$\alpha$ and AR (Figure 4), suggesting that HB-EGF is a major EGF family ligand, and is involved in tumour growth and OVCA extension.

To elucidate the relationship between EGFR ligands and clinical outcome, the amounts of EGFR ligands in peritoneal fluid were compared between before and after chemotherapy. Of the six cases examined, three cases showed a good response to neo-adjuvant chemotherapy and a marked reduction in tumour size and peritoneal fluid. In these cases, computed tomography indicated the disappearance of the tumour in the abdomen with six courses of chemotherapy. The other three cases did not respond to neo-adjuvant chemotherapy and there was no marked effect on tumour growth or the volume of peritoneal fluid. The levels of HB-EGF were dramatically reduced in the former cases, but were slightly increased in the latter ones (Figure 5A). No significant changes in TGF-$\alpha$ and AR were observed between pre- and post-chemotherapy (Figure 5B and C). These results suggest that HB-EGF levels in peritoneal fluid might reflect the response to chemotherapy.

## DISCUSSION

In this study, we have shown the following: (1) HB-EGF levels in peritoneal fluid were elevated at all stages and at recurrence, and levels of HB-EGF were sufficient to proliferate and to allow survival of OVCA cells, whereas the levels of the other five EGFR ligands in peritoneal fluid had little effect on the proliferation of OVCA cells. (2) Cell proliferation of OVCA cells was stimulated by the addition of HB-EGF, but not LPA, in *in vitro* study. (3) Changes in the amount of HB-EGF were reflected by therapeutic efficacy in OVCA patients. Taken together, the present study suggests that HB-EGF plays a pivotal role in tumour growth and extension of OVCA. In this study, however, cell proliferative activities in SKOV3, RMG-1, or OVMG1 cells, which were mediated by peritoneal fluid from OVCA patients, were not always dependent on the expression of EGFR or ErbB-4. It remains open to debate how EGFR or ErbB-4 is involved in the cell proliferation mediated by peritoneal fluid in OVCA patients.

Among the members of EGF family growth factors, HB-EGF, AR, and betacellulin have heparin-binding properties (Raab and Klagsbrun, 1997; Iwamoto and Mekada, 2000; Strachan *et al*, 2001). Heparin-binding epidermal growth factor is also known to have a broad spectrum of biological activities including mitogenic activity, chemotaxis, adhesion, and angiogenesis (Raab and Klagsbrun, 1997; Iwamoto and Mekada, 2000). Increasing evidence indicates that HB-EGF is involved in various pathophysiological disorders. Recently, it has been shown that EGFR is transactivated by a variety of stimuli through the ectodomain shedding of EGFR ligands, and that HB-EGF plays a central role in this process (Prenzel *et al*, 1999). Lysophosphatidic acid and other ligands for G protein coupled receptors (GPCR) also transactivate EGFR through ectodomain shedding of HB-EGF or AR (Prenzel *et al*, 1999; Umata *et al*, 2001; Gschwind *et al*, 2003). In OVCA, LPA has been

**Table 2** Concentrations of HB-EGF, TGF-$\alpha$, and amphiregulin, and cell proliferation properties in peritoneal fluid

| | Concentration of EGF ligands (pg ml$^{-1}$, mean ± s.d.) | | | Proliferation-promoting activities (mean ± s.d.) | |
|---|---|---|---|---|---|
| Variable | HB-EGF | TGF-$\alpha$ | Amphiregulin | [$^3$H]Thymidine incorporation (c.p.m.) | WST-1 assay (abs.) |
| Normal ovary ($N=18$) | 483 ± 495 | 11.12 ± 13.01 | 98 ± 236 | 9216 ± 5777 | 0.12 ± 0.11 |
| Ovarian cyst ($N=18$) | 653 ± 616 | 7.37 ± 3.67 | 186 ± 322 | 8990 ± 5381 | 0.26 ± 0.18 |
| Ovarian cancer, stage Ia ($N=10$) | 3090 ± 2286* | 7.45 ± 4.01 | 214 ± 183 | 21 747 ± 8678** | 0.71 ± 0.29*** |
| Ovarian cancer, stage Ic–II ($N=13$) | 2132 ± 1394* | 8.33 ± 7.47 | 203 ± 220 | 18 654 ± 4988** | 0.76 ± 0.33*** |
| Ovarian cancer, stage III–IV ($N=30$) | 2053 ± 1204* | 5.14 ± 0.62 | 225 ± 755 | 24 556 ± 10 152** | 0.86 ± 0.66*** |
| Ovarian cancer, Recurrence ($N=10$) | 2544 ± 1098* | 2.01 ± 5.12 | 212 ± 175 | 21 035 ± 9755** | 0.78 ± 0.28*** |

*$P<0.01$ for comparison of HB-EGF level *vs* normal ovary. **$P<0.01$ for comparison of c.p.m. count *vs* normal ovary. ***$P<0.01$ for comparison of absorbance *vs* normal ovary.

**Figure 1** Cell proliferation activity mediated by peritoneal fluid in patients with a normal ovary (NO), an ovarian cyst (OVC), or ovarian cancer (OVCA). (**A**) Expression of EGFR and ErbB-4 protein in SKOV3, RMG-1, and OVMG1 cells. Lanes 1 and 4: SKOV3 cells. Lanes 2 and 5: RMG-1 cells. Lanes 3 and 6: OVMG1 cells. (**B**) The value of absorbance in the WST-1 assay in SKOV3 cells incubated with patients' peritoneal fluid from an NO, an OVC, and an OVCA at clinical stages Ia, Ic-II, III–IV, and recurrence. Closed circles indicate the value of absorbance in each patient. Horizontal lines indicate mean values. The *P*-value represents comparison with the levels of patients with an NO and an OVC. (**C**) The [$^3$H]thymidine incorporation in SKOV3 cells incubated with patients' peritoneal fluid of a NO, an OVC, and an OVCA at clinical stages Ia, Ic-II, III–IV, and recurrence. Closed circles indicate the value of [$^3$H]thymidine incorporation in each patient. Horizontal lines indicate mean values. The *P*-value represents comparison with the levels of patients with a normal ovary and an ovarian cyst. (**D**) Alterations in the [$^3$H]thymidine incorporation of an ovarian cancer patient's peritoneal fluid by anti-EGFR ligand antibodies or an anti-EGFR antibody. A bar indicates the mean value and standard errors. The *P*-value represents comparison with the levels of patients in the absence of inhibitory antibodies.

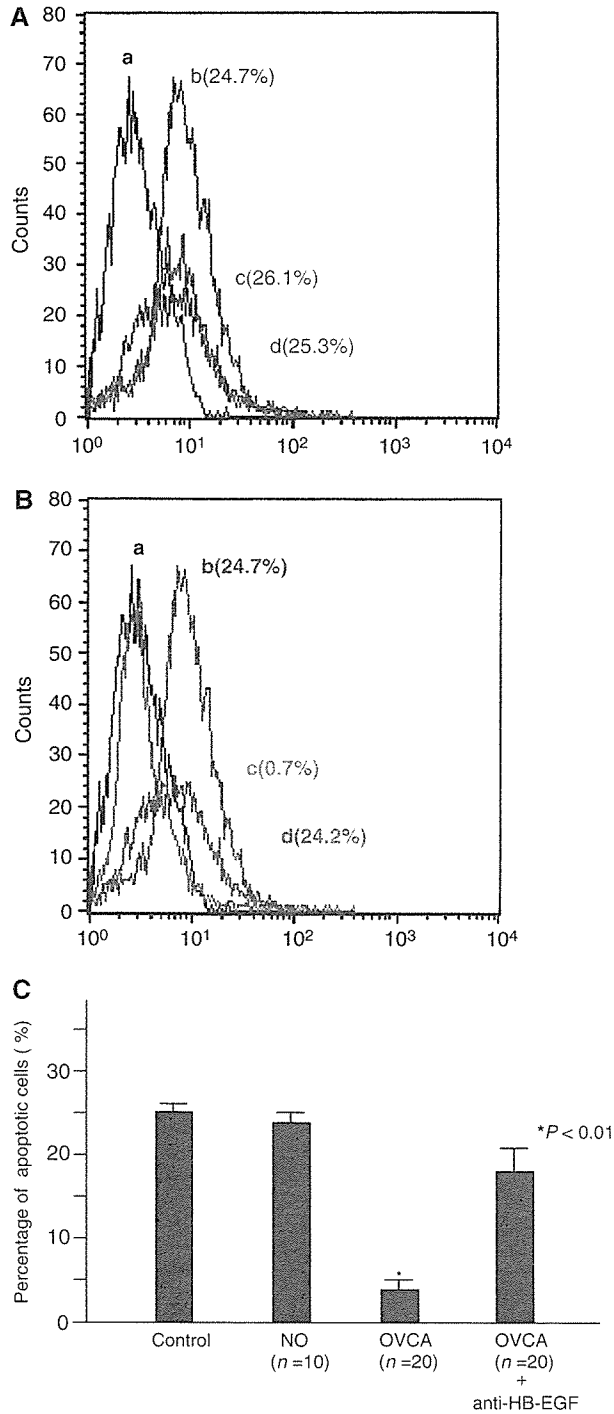


**Figure 2** Cell survival activity mediated by peritoneal fluid in patients with a normal ovary or ovarian cancer. Flow cytometric analysis for apoptotic cells in SKOV3 cells after incubation with peritoneal fluid of a normal ovary (**A**) and ovarian cancer (**B**). Control (a: black line). Under serum-free condition (b: green line). Incubation with 10% peritoneal fluid in the absence (c: red line) or presence (d: blue line) of an inhibitory antibody against HB-EGF. Each percentage indicates the ratio of apoptotic cells in SKOV3 cells. (**C**) Alteration in the percentage of apoptotic cells after incubation with the peritoneal fluid from a normal ovary or ovarian cancer. A bar indicates the mean value and standard errors. The *P*-value represents comparison with the levels of patients with a normal ovary.

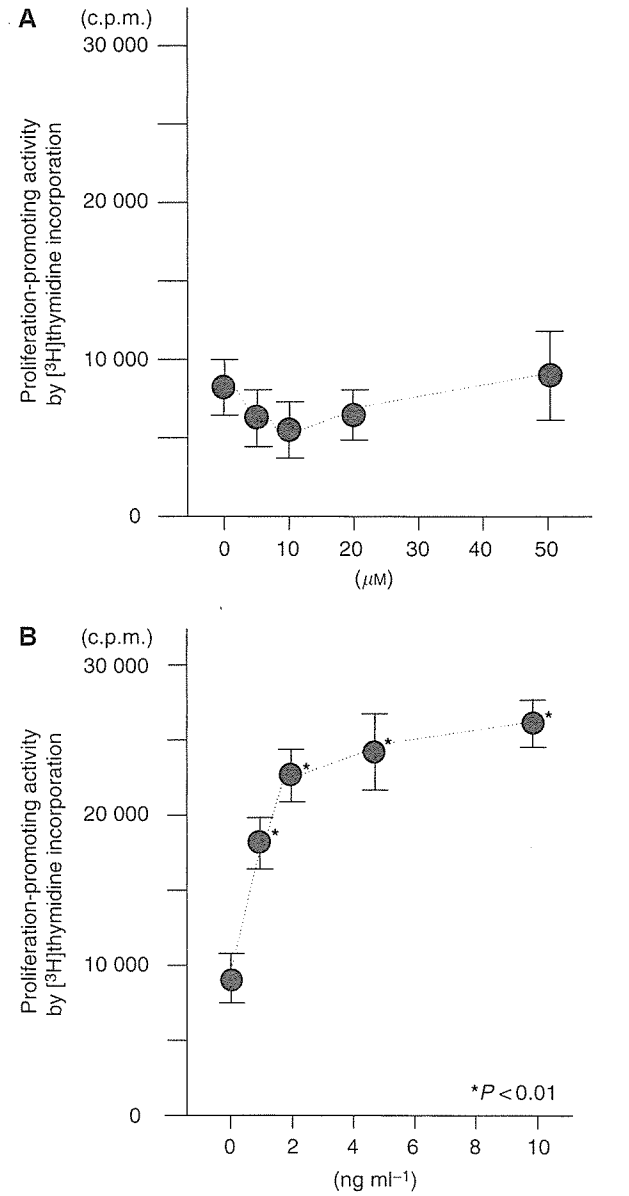


**Figure 3** Mitogenic activity of LPA (**A**) and HB-EGF (**B**) in the presence of peritoneal fluid. Each point indicates the mean and standard deviation of [$^3$H]thymidine incorporation. The *P*-value represents comparison with the levels of [$^3$H]thymidine incorporation incubated in the medium containing peritoneal fluid of a patient with a normal ovary.

identified as a candidate for an OCAF (Xu *et al*, 1995; Westermann *et al*, 1998; Xiao *et al*, 2001). In our study, LPA did not stimulate SKOV3 cell proliferation in the presence of peritoneal fluid of NO patients; however, the effect of LPA might be dependent on the cell system. In contrast, HB-EGF stimulated SKOV3 cell proliferation in the same culture conditions. Therefore, it is likely that LPA is an OCAF, but it stimulates OVCA cell proliferation by inducing the ectodomain shedding of HB-EGF, rather than directly acting by itself on cancer cells.

In OVCA, LPA regulates the production of LPA itself through the activation of phospholipase D and phospholipase A2 (Eder *et al*, 2000). Similarly, HB-EGF induces HB-EGF gene expression itself by activating mitogenic properties (Tan *et al*, 1994). In addition, LPA and HB-EGF appear to influence their reciprocal production. Lysophophatidic acid can enhance

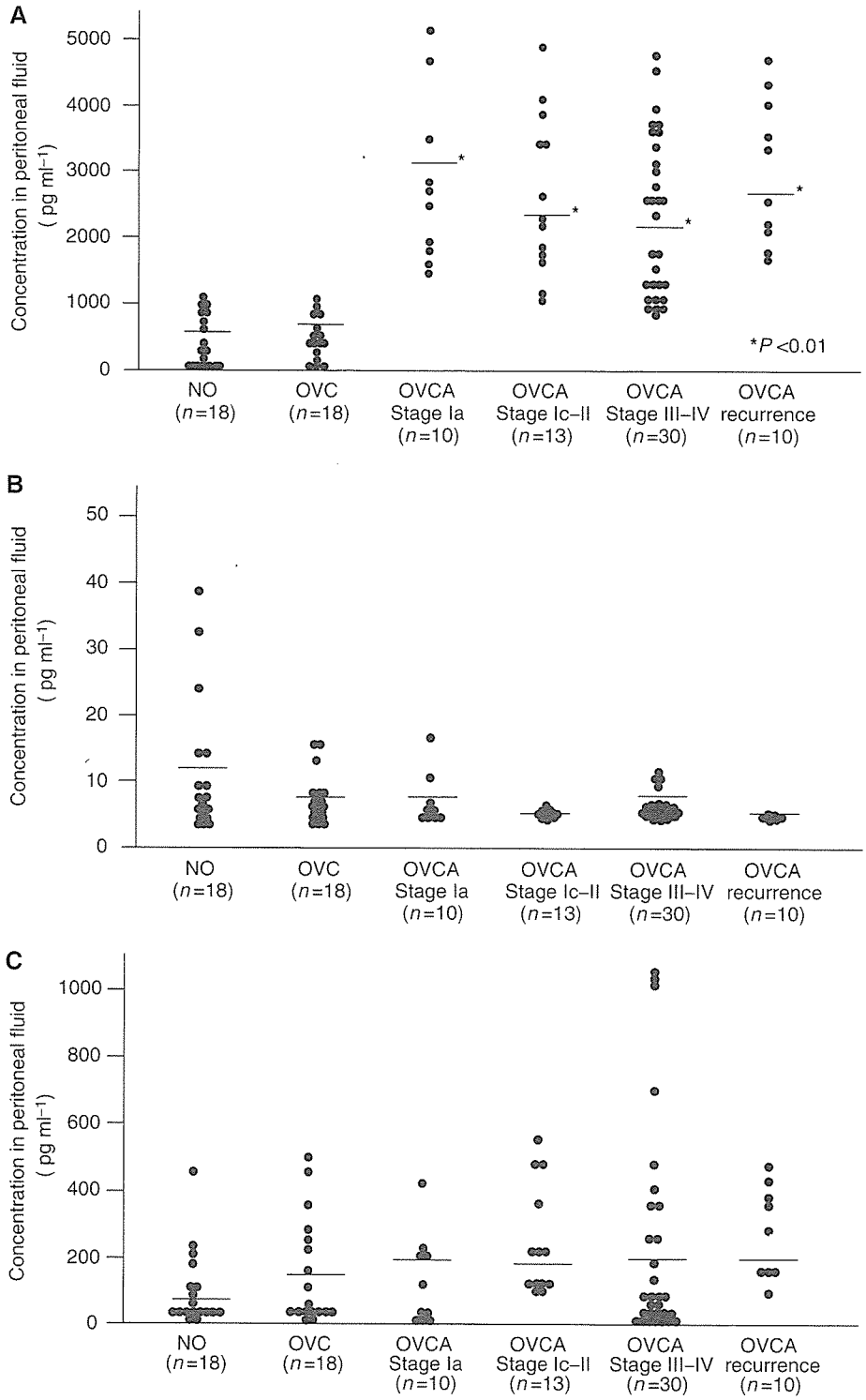


**Figure 4** Distribution of HB-EGF (**A**), TGF-α (**B**), and AR (**C**) concentration in peritoneal fluid among patients with a normal ovary (NO), an ovarian cyst (OVC), or ovarian cancer (OVCA) at clinical stages Ia, Ic-II, III–IV, and recurrence. Closed circles indicate the value of EGFR ligand concentration in each patient. Horizontal lines indicate mean values. The *P*-value represents comparison with the levels of patients with an NO or an OVC.

the gene expression of HB-EGF (Goetzl *et al*, 1999), as well as induce the ectodomain shedding of HB-EGF (Prenzel *et al*, 1999; Umata *et al*, 2001). Heparin-binding epidermal growth factor activates EGFR, and the activated EGFR enhances the activity of phospholipase D, which in turn causes the production of LPA (Yeo and Exton, 1995). Considering this evidence as a basis, HB-EGF and LPA might collaborate in inducing cell proliferation and in amplifying their own production. In this study, we showed that HB-EGF is elevated in the ascitic fluid of OVCA patients even at an early stage. Lysophophatidic acid may contribute to the production of HB-EGF, especially in an early phase of OVCA.

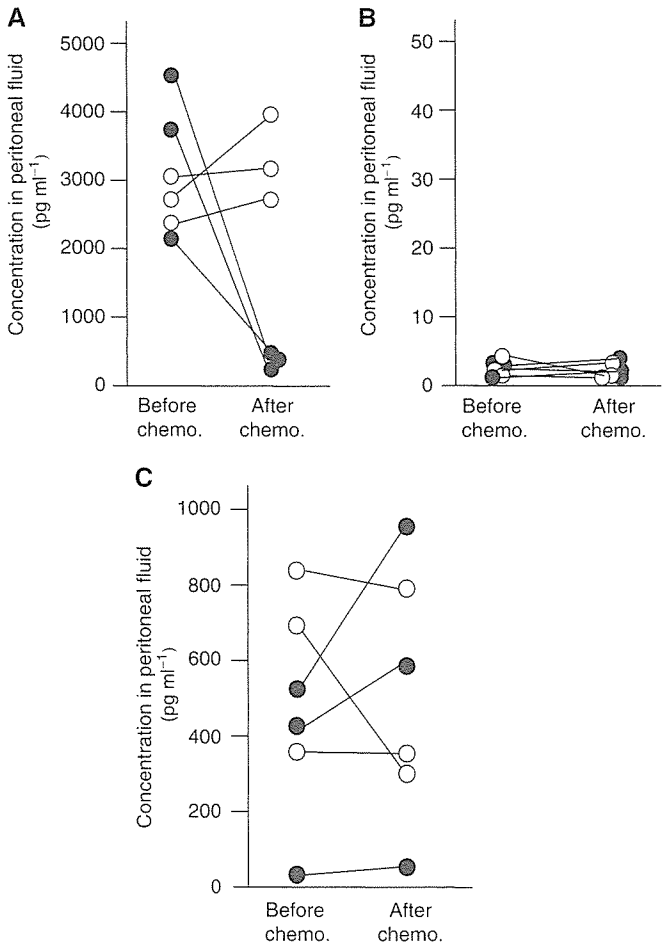


**Figure 5** Changes in concentrations of HB-EGF (**A**), TGF-$\alpha$ (**B**), and AR (**C**) in the peritoneal fluid among patients with ovarian cancer between pre- and post-chemotherapy. Open circles indicate the concentration of each peritoneal fluid from chemotherapy-non-responding patients. Closed circles indicate the concentration of each peritoneal fluid from chemotherapy-responding patients.

Heparin-binding epidermal growth factor in peritoneal fluid is generated mainly from cancer cells and peritoneal mesothelial cells, which have the same origin as coelomic epithelium of the NO. Our study showed that HB-EGF levels were already elevated even in the ascitic fluid of patients with stage Ia OVCA, whereas OVCA cells are enclosed within the cyst wall. This suggests that HB-EGF is not secreted from cancer tissues in an early stage. In peritoneal mesothelial cells, HB-EGF is constitutively expressed and produced by cytokine stimulation (Jayne *et al*, 2000). Therefore, it is possible to speculate that during early OVCA, mainly peritoneal mesothelial cells produce HB-EGF in the peritoneal fluid by stimulation of a variety of cytokines or by LPA. In advanced stages of OVCA, however, the HB-EGF levels in the peritoneal fluid appear to be correlated with the tumour state in the peritoneal cavity, as HB-EGF levels of patients' fluids were largely reduced after chemotherapy in chemotherapy-responding cases. Therefore, in advanced OVCA, both cancer and peritoneal mesothelial cells might produce HB-EGF.

These results are the first demonstration of HB-EGF as an OCAF. Heparin-binding epidermal growth factor is known to enhance cell motility as well as cell proliferation. Therefore, elevated HB-EGF in peritoneal fluid may contribute to not only survival and proliferation of cancer cells, but also to their dissemination into the peritoneal cavity. It is easier to measure HB-EGF levels in peritoneal fluid compared with LPA, suggesting that HB-EGF is a promising bioactive marker of OVCA. For therapy, relevant LPA antagonists have yet to be developed, while Iressa, a specific EGFR tyrosine-kinase inhibitor, is not effective in OVCA (Baselga *et al*, 2002). Thus, the development of therapeutic tools against HB-EGF would allow the exploration of novel targeting therapies for OVCA.

## ACKNOWLEDGEMENTS

This work was supported in part by the grant-in-aid for cancer research from the Ministry of Health and Welfare of Japan (Number: 16591667) for SM and the grants-in-Aid for Scientific Research on Priority Areas from the Ministry of Education, Culture, Sports, Science and Technology, Grant (Number: 14032202) for EM.

## REFERENCES

Baselga J, Rischin D, Ranson M, Calvert H, Raymond E, Kieback DG, Kaye SB, Gianni L, Harris A, Bjork T, Aberbuch SD, Feyereislova A, Swaisland H, Rojo F, Albanell J (2002) Phase I safety, pharmacokinetic, and pharmacodynamic trial of ZD1839, a selective oral epidermal growth factor receptor tyrosine kinase inhibitor, in patients with five selected solid tumor types. *J Clin Oncol* **20:** 4292–4302

D'Antonio A, Losito S, Pignata S, Grassi M, Perrone F, De Luca A, Tambaro R, Bianco C, Gullick WJ, Johnson GR, Iaffaioli VR, Salomon DS, Normanno N (2002) Transforming growth factor alpha, AR and cripto-1 are frequently expressed in advanced human ovarian carcinomas. *Int J Oncol* **21:** 941–948

Eder AM, Sasagawa T, Mao M, Aoki J, Mills GB (2000) Constitutive and lysophosphatidic acid (LPA)-induced LPA production: role of phospholipase D and phospholipase A2. *Clin Cancer Res* **6:** 2482–2491

Fischer OM, Hart S, Gschwind A, Ullrich A (2003) EGFR signal transactivation in cancer cells. *Biochem Soc Trans* **31:** 1203–1208

Goetzl EJ, Kong Y, Kenney JS (1999) Lysophospholipid enhancement of human T cell sensitivity to diphtheria toxin by increased expression of heparin-binding epidermal growth factor. *Proc Assoc Am Physicians* **111:** 259–269

Gschwind A, Hart S, Fischer OM, Ullrich A (2003) TACE cleavage of proAR regulates GPCR-induced proliferation and motility of cancer cells. *EMBO J* **22:** 2411–2421

Iwamoto R, Higashiyama S, Mitamura T, Taniguchi N, Klagsbrun M, Mekada E (1994) Heparin-binding EGF-like growth factor, which acts as the diphteria toxin receptor, forms a complex with membrane protein DRAP27/CD9, which up-regulates functional receptors and diphteria toxin sensitivity. *EMBO J* **13:** 2322–2330

Iwamoto R, Mekada E (2000) Heparin-binding EGF-like growth factor: a juxtacrine growth factor. *Cytokine Growth Factor Rev* **11:** 335–344

Jayne DG, Perry SL, Morrison E, Farmery SM, Guillon PJ (2000) Activated mesothelial cells produce heparin-binding growth factors: implications for tumor metastases. *Br J Cancer* **82:** 1233–1238

Mills GB, May C, McGill M, Roifman CM, Mellers A (1998) A putative new growth factor in ascitic fluid from ovarian cancer patients: identification, characterization, and mechanism of action. *Cancer Res* **48:** 1066–1071

Mills GB, Moolenaar WH (2003) The emerging role of lysophosphatidic acid in cancer. *Nat Rev Cancer* **3:** 582–591

Miyamoto S, Hirata M, Yamazaki A, Kageyama T, Hasuwa H, Mizushima H, Tanaka Y, Yagi H, Sonoda K, Kai M, Kanoh H, Nakano H, Mekada E (2004) Heparin-binding EGF-like growth factor and the LPA-induced ectodomain shedding pathway is a promising target for the therapy of ovarian cancer. *Cancer Res* **64:** 5720–5727

Morimoto H, Safrit JT, Bonavida J (1991) Synergistic effect of tumor necrosis factor-alpha- and diphteria toxin-mediated cytotoxicity in

sensitive and resistant human ovarian tumor cell lines. *J Immunol* **147:** 2609–2616

Morishige K, Kurachi H, Amemiya K, Fujita Y, Yamamoto T, Miyake A (1991) Evidence for the involvement of transforming growth factor α and epidermal growth factor receptor autocrine growth mechanism in primary human ovarian cancers *in vitro*. *Cancer Res* **51:** 5322–5328

Normanno N, Bianco C, De Luca A, Maiello MR, Salomon DS (2003) Target-based agents against ErbB receptors and their ligands: a novel approach to cancer treatment. *Endocr Relat Cancer* **10:** 1–21

Penson RT, Shannon KE, Sharpless NE, Seiden MV (1998) Ovarian cancer an update on genetics and therpapy. *Compr Ther* **24:** 477–487

Prenzel N, Zwick E, Daub H, Leserer M, Abraham R, Wallasch C, Ullrich A (1999) EGF receptor transactivation by G-protein-coupled receptors requires metalloproteinase cleavage of proHB-EGF. *Nature* **402:** 884–888

Raab G, Klagsbrun M (1997) Heparin-binding EGF-like growth factor. *Biochim Biophys Acta* **1333:** F179–F199

Salomon DS, Brandt R, Ciardiello F, Normanno M (1995) Epidermal growth factor-related peptides and their receptors in human malignancies. *Crit Rev Oncol Hematol* **19:** 183–232

Scambia G, Benedetti Panci P, Battaglia F, Ferrandina G, Baiocchi G, Greggi S, De Vincenzo R, Mancuso S (1992) Significance of epidermal growth factor receptor in advanced ovarian cancer. *J Clin Oncol* **10:** 529–535

Strachan L, Murison JG, Prestidge RL, Sleeman MA, Watson JD, Kumble KD (2001) Cloning and biological activity of epigen, a novel member of the epidermal growth factor superfamily. *J Biol Chem* **25:** 18265–18271

Tan MS, Tsai JC, Lee YJ, Chen HC, Shin SJ, Lai YH, Parrella MA, Bianchi C, Higashiyama S, Endege W, Lee ME, Tsai JH (1994) Induction of heparin-binding epidermal growth factor-like growth factor mRNA by protein kinase C activators. *Kidney Int* **46:** 690–695

Umata T, Hirata M, Takahashi T, Ryu F, Shida S, Takahashi Y, Tsuneoka M, Miura Y, Masuda M, Horiguchi Y, Mekada E (2001) A dual signaling cascade that regulates the ectodomain shedding of heparin-binding epidermal growth factor-like growth factor. *J Biol Chem* **276:** 30475–30482

Westermann AM, Beijnen JH, Moolenaar WH, Rodenhuis S (1997) Growth factors in human ovarian cancer. *Cancer Treat Rev* **23:** 113–131

Westermann AM, Havik E, Postma FR, Beijnen JH, Dalesio O, Moolenaar WH, Rodenhuis S (1998) Malignant effusion contain ; lysophosphatidic acid (LPA) -like activity. *Ann Oncol* **9:** 437–442

Xiao YJ, Schwartz B, Washington M, Kennedy A, Webster K, Belinson J, Xu Y (2001) Electrospray lonization mass spectrometry analysis of lysophospholipids in human ascitic fluids: comparison of the lysophospholipid contents in malignant *vs* nonmalignant ascitic fluids. *Anal Biochem* **290:** 302–313

Xu Y, Gaudette DC, Boynton JD, Frankel A, Fang XJ, Sharma A, Hurteau J, Casey G, Goodbody A, Mellors A, Holub BJ, Mills GB (1995) Characterization of an ovarian cancer activating factor in ascites from ovarian cancer patients. *Clin Cancer Res* **1:** 1223–1232

Yeo EJ, Exton JH (1995) Stimulation of phospholipase D by epidermal growth factor requires protein kinase C activation in Swiss 3T3 cells. *J Biol Chem* **270:** 3980–3988

# Adenovirus-Mediated *Calponin h1* Gene Therapy Directed against Peritoneal Dissemination of Ovarian Cancer: Bifunctional Therapeutic Effects on Peritoneal Cell Layer and Cancer Cells

Tomonori Ogura,[1] Hiroaki Kobayashi,[1] Yousuke Ueoka,[1] Kaoru Okugawa,[1] Kiyoko Kato,[2] Toshio Hirakawa,[1] Shigenari Hashimoto,[3,4] Shun'ichiro Taniguchi,[4] Norio Wake,[1] and Hitoo Nakano[1]

**Abstract**

**Purpose:** Calponin h1 (CNh1), one of the family of actin-binding proteins, stabilizes the filaments of actin and modulates various cellular biological phenotypes. Recent studies revealed the close correlation between the invasive tumor spread and the reduced expression of CNh1 and α-smooth muscle actin in the surrounding stromal cells. The purpose of this study is to evaluate the efficacy of i.p. *CNh1* gene therapy against peritoneal dissemination of ovarian cancer.

**Experimental Design:** We used an adenoviral vector to induce the *CNh1* gene into peritoneal cells and ovarian cancer cells as a means of enhancing or inducing the expression of α-smooth muscle actin as well as CNh1. The efficacy of gene transfer was examined by *in vitro* cell culture and *in vivo* animal experiments.

**Results:** The formation of longer and thicker actin fibers was observed in each transfected cell line, and the localization of these fibers coincided with that of externally transducted *CNh1*. With respect to changes in cell behavior, the *CNh1*-transfected peritoneal cells acquired an ability to resist ovarian cancer-induced shrinkage in cell shape; thus, cancer cell invasion through the monolayer of peritoneal cells was inhibited. In addition, *CNh1*-transfected ovarian cancer cells showed suppressed anchorage-independent growth and invasiveness, the latter of which accompanied impaired cell motility. The concomitant *CNh1* transfection into both peritoneal cells and ovarian cancer cells produced an additive inhibitory effect with respect to cancer cell invasion through the peritoneal cell monolayer. By *in vivo* experiments designed to treat nude mice that had been i.p. inoculated with ovarian cancer cells, we found that the i.p. injected *CNh1* adenovirus successfully blocked cancer-induced morphologic changes in peritoneal cell surface and significantly prolonged the survival time of tumor-bearing mice. Moreover, *CNh1* adenovirus could successfully enhance the therapeutic effect of an anticancer drug without increase in side effects.

**Conclusions:** Thus, *CNh1* gene therapy against peritoneal dissemination of ovarian cancer is bifunctionally effective (i.e., through inhibitory effects on the infected peritoneal cell layers that suppress cancer invasion and through direct antitumor effects against invasion and growth properties of cancer cells).

**Authors' Affiliations:** [1]Department of Gynecology and Obstetrics, Graduate School of Medical Sciences, and [2]Department of Molecular Genetics, Division of Molecular and Cell Therapeutics, Medical Institute of Bioregulation, Kyushu University, Fukuoka, Japan; [3]Division of Otorhinolaryngology, Shinshu University School of Medicine, Matsumoto, Japan; and [4]Department of Molecular Oncology, Institute on Aging and Adaptation, Shinshu University Graduate School of Medicine, Matsumoto, Japan

Received 3/20/06; revised 6/8/06; accepted 6/15/06.

**Grant support:** Ministry of Education, Culture, Sports, Science, and Technology, Japan scientific research grants 14570117, 15390509, 16659100, 1690960, and 17591747.

The costs of publication of this article were defrayed in part by the payment of page charges. This article must therefore be hereby marked *advertisement* in accordance with 18 U.S.C. Section 1734 solely to indicate this fact.

**Note:** T. Ogura and H. Kobayashi contributed equally to this work.

**Requests for reprints:** Hiroaki Kobayashi, Department of Gynecology and Obstetrics, Graduate School of Medical Sciences, Kyushu University, Maidashi 3-1-1, Higashi-ku, Fukuoka 812-8582, Japan. Phone: 81-92-642-5395; Fax: 81-92-642-5414; E-mail: koba@med.kyushu-u.ac.jp.



doi:10.1158/1078-0432.CCR-06-0674

Peritoneal dissemination is a main obstacle to improve the prognosis of ovarian cancer patients. The process to establish peritoneal implants is as follows: cancer cells are released from the primary ovarian tumor site into the abdominal cavity, attach to and invade through the peritoneal mesothelial layer, and proliferate as "implanted" tumors. For these processes, dynamic cytoskeletal remodeling is essential not only for the tumor cells but also for the peritoneal cells. A recent study analyzing several adenocarcinomas of various organs has shown that nine genes in metastatic sites were universally down-regulated compared with their primary tumor counterparts (1). Surprisingly, four of these nine genes are associated with the actin cytoskeleton [i.e., α-actin, myosin light and heavy chain kinases, and calponin h1 (CNh1)]. As such, this seems to be a reflection of the importance of actin cytoskeletal disorganization in the metastatic process.

CNh1 is a 34-kDa actin-binding protein that was originally isolated from chicken gizzard (2). CNh1 is mainly expressed in

smooth muscle cells in contrast to other two isoforms of calponin h2 and acidic calponin, which are mainly expressed in nonmuscle cells and the brain, respectively (3–5). CNh1 has an ability to (*a*) bind to the thin filament of actin, tropomyosin, and calmodulin (2, 6, 7); (*b*) inhibit the actin-activated myosin Mg-ATPase (8); (*c*) inhibit $Ca^{2+}$-dependent mobility of actin on immobilized myosin (9); and (*d*) induce conformational changes in actin filament (F-actin; ref. 10). Therefore, CNh1 is thought to play an essential role in organizing stable actin stress fibers. We have confirmed previously that (*a*) the expression of α-smooth muscle actin (α-SMA) decreased in blood vessels located at the proximity of ovarian cancer nests (11) and in fibroblasts and peritoneal mesothelia cultured in the presence of ovarian cancer cell–derived factors[5] and (*b*) the decrease in CNh1 and α-SMA expression was seemingly attributed to the secreted factors, including platelet-derived growth factor derived from cancer cells (12, 13). *CNh1* knockout mice showed the enhanced peritoneal dissemination and lung metastasis by malignant melanoma cells through their highly fragile peritoneum and vascular wall in contrast to the wild-type mice. However, *CNh1* gene transfection into the peritoneal cells of knockout mice could successfully inhibit cancer cell invasion into peritoneal cell layer (14, 15). The efficacy of *CNh1* transfection into cancer cells themselves was also reported by our colleagues; both cell growth and tumorigenicity were significantly inhibited in *CNh1*-transfected leiomyosarcoma cells (16) and fibrosarcoma cells (17).

Based on these observations, we hypothesized that CNh1 has bifunctional effects (i.e., an enhancement of peritoneal defense ability on the one hand and a direct inhibitory effect against for ovarian cancer cells on the other). The purpose of this study was to examine the effects of *CNh1* gene transduction into both cancer cells and peritoneal cells with respect to inhibiting peritoneal dissemination of ovarian cancers.

## Materials and Methods

*Cell lines and animals.* Four i.p. transplantable (SHIN-3, MCAS/as, OVAS-21/om, and SKOV3i.p.1) and a poorly transplantable (SKOV3) human ovarian cancer cell lines were used in this study. SHIN-3, a serous adenocarcinoma cell line, was purchased from Scienstaff Co. Ltd. (Nara, Japan). MCAS/as and OVAS-21/om were established from ascites and omentum of nude mice i.p. inoculated by their parental cell lines of MCAS (mucinous adenocarcinoma) and OVAS-21 (clear cell adenocarcinoma), respectively. Both cell lines were generous gifts from Drs. S. Minami and Y. Yoshikawa (Department of Obstetrics and Gynecology, University of Tsukuba, Japan) and M. Noguchi (Department of Molecular Pathology, University of Tsukuba). SKOV3i.p.1, provided by Dr. I.J. Fidler (Department of Cancer Biology, M.D. Anderson Cancer Center, Houston, TX), was established as an i.p. transplantable subline from a parental adenocarcinoma cell line of SKOV3 (18). A Chinese hamster peritoneal cell line, CCL14, was purchased from American Type Culture Collection (Manassas, VA). FK is a primary culture of human peritoneal cells, which were obtained from the surgical specimen of omentum under the patient's consent in Department of Obstetrics and Gynecology, Kyushu University Hospital. Each cell line was cultured in RPMI 1640 (Invitrogen, Carlsbad, CA) supplemented with 10% fetal bovine serum, 100 μg/mL streptomycin, 100 units/mL penicillin G, and 2.5 μg/mL amphotericin B at 37°C in 5% $CO_2$ in air.

Female athymic BALB/c *nu/nu* mice between 6 and 8 weeks old (Charles River Japan, Atsugi, Japan) were used for *in vivo* experiments. The mice were maintained in a laminar-flow cabinet under specific pathogen-free conditions while receiving standard feed and water *ad libitum*. Our experiments were reviewed by the Committee of Ethics in Animal Experiments in the Graduate School of Medical Sciences, Kyushu University, and the Law (no. 105) and the Notification (no. 6) of the Government.

*Construction of recombinant adenovirus and adenoviral gene transfection into cultured cells.* Recombinant adenovirus was inserted with the *CNh1*-green fluorescent protein (GFP) fusion gene (AdCNh1) or with the *GFP* gene only (AdGFP, control vector) as described previously (15). Briefly, *CNh1-GFP* fusion gene was produced by inserting human *CNh1* gene into pEGFP-C2 (Clontech, Palo Alto, CA), and then subcloned under the transcriptional control of CAG promoter/enhancer in cosmid vector pAxCAwt (adenovirus expression kit, TaKaRa, Japan; Fig. 1). The recombinant was continued in 293 cells by four times infection and high titer virus was obtained. Adenoviral infection into the cells was carried out by incubating subconfluent cells with adenoviral vectors ($2 \times 10^7$ plaque-forming units/15-mm dish) for 2 hours in RPMI 1640 at 37°C. Cells were then washed twice with PBS and the medium was changed into RPMI 1640 containing 10% fetal bovine serum. After 24 hours of incubation, cells were used for immunofluorescent cell staining and colony-forming assay. For Western blot analysis, *in vitro* invasion assay, and cell motility assay, cells were used after 4 days of additional incubation.

*Plasmid gene transfection into cultured cells.* A human *CNh1* cDNA was subcloned into a pCMV-neo-Bam vector as described previously (17). Either *CNh1* cDNA construct or control vector (20 μg) was transfected into SKOV3 cell line by Lipofectin method. Transfected cells were maintained at 37°C in a complete RPMI 1640. After 14 days, the G418-resistant clones were harvested and established.

*Western blot analysis.* Subconfluently growing cells were lysed in a lysis buffer [50 mmol/L Tris-HCl (pH 8.0), 0.25 mol/L NaCl, 0.5% NP40, 1 mmol/L phenylmethylsulfonyl fluoride, 10 μg/mL aprotinin, 1 μg/mL leupeptin]. After centrifugation at 13,000 × *g* for 10 minutes to remove debris, equal protein amount of cell lysates was separated on

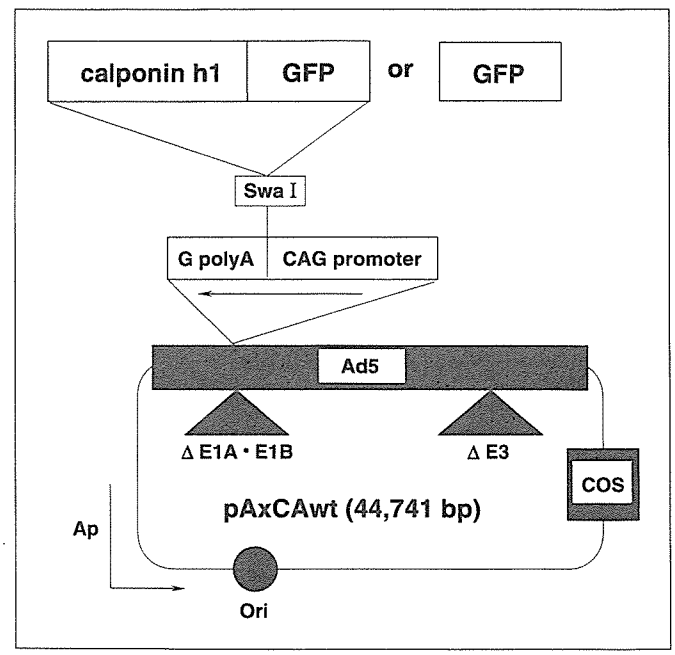


Fig. 1. Construction of *CNh1-GFP* recombinant adenovirus vector (AdCNh1) and its control *GFP* vector (AdGFP).

[5] Unpublished observations.

SDS-PAGE and transferred onto nitrocellulose membranes. The membranes were blocked in TBS [10 mmol/L Tris-HCl (pH 7.4), 150 mmol/L NaCl, 0.05% Tween 20] containing 5% nonfat dry milk for 1 hour at room temperature and washed in TBS-Tween 20 for 5 minutes. The blots were incubated with anti-human CNh1 monoclonal antibody (Sigma, St. Louis, MO), anti-human α-SMA monoclonal antibody (Progen, Queensland, Australia), anti-β-actin monoclonal antibody (Sigma), antibody (Santa Cruz Biotechnology, Inc., CA) for 2 hours at room temperature. After washing, the blots were reacted with their respective secondary antibodies (Amersham, Piscataway, NJ) and analyzed with enhanced chemiluminescence system (Amersham). All primary antibodies are informed to detect CNh1 protein stably even in murine tissues.

*Immunofluorescent cell staining for F-actin.* Cells were washed with PBS and fixed in 3.7% formaldehyde solution in PBS for 10 minutes at room temperature. After permeabilization with 1% Triton X-100, the rhodamine-phalloidin (Molecular Probes, OR) diluted with 0.1% bovine serum albumin in PBS was added and incubated at room temperature for 20 minutes. F-actin and GFP were observed with confocal laser scanning microscope using specific filters for rhodamine and FITC, respectively.

*Soft-agar colony-forming assay.* After 24 hours of infection with AdCNh1 or AdGFP, $10^4$ cells were seeded into the complete medium, including 0.3% agar, and placed over a hardened 0.5% agar base layer in 60-mm dishes. Visible colonies were counted in triplicate after 14 days of incubation to evaluate the anchorage-independent cell growth.

*Tumorigenicity in nude mice.* Single-cell suspension containing $10^7$ SKOV3 cells with or without plasmid transfection was i.m. injected into the thigh of nude mice. The mice were observed weekly, and tumor growth was evaluated by measuring the thickness of the inoculated thigh.

*Cell motility assay.* Cell motility was determined using Transwell chambers inserted with 8-μm pore size membrane (Costar, Corning, NY) according to the method described previously (19). Each lower compartment of Transwell chambers was filled with a conditioned medium as a source of chemoattractant, which was a supernatant of confluently cultured NIH3T3 cells in DMEM supplemented with 10% fetal bovine serum for 24 hours. Single-cell suspension containing $5 \times 10^4$ cells infected by AdCNh1 or AdGFP in 100 μL RPMI 1640 with 0.1% bovine serum albumin was placed in its upper compartment. The cells were incubated for 12 hours at 37°C, fixed with methanol, and stained with H&E. Cells on the upper surface of the filter were removed with a cotton swab, and cells that migrated to the lower surface were counted by six fields of a light microscope at ×200 magnification.

**In vitro** *invasion assay.* *In vitro* invasion assay was done using Transwell chambers with 8-μm pore membrane coated with 20 μg Matrigel (Becton Dickinson Collaborative Research, Bedford, MA) as described previously (20). Conditioned medium prepared by NIH3T3 cells was placed in the lower compartment. Single-cell suspension containing $10^5$ cells in 100 μL RPMI 1640 containing 10% fetal bovine serum was placed in the upper compartment and incubated for 24 hours. The subsequent procedures were the same as those of the cell motility assay.

*Assay for invasion through the peritoneal cell monolayer.* Single-cell suspensions containing $10^6$ cancer cells infected with AdCNh1 or AdGFP were plated on the monolayer of CCL14 peritoneal cells infected with AdCNh1 or AdGFP, and cultured for additional 24 hours. The number of colonies derived from a penetrated cancer cell was counted by six fields of a phase-contrast microscope at ×400 magnification.

*Therapeutic experiments against i.p. inoculated ovarian cancer cells.* One day after the inoculation of $10^6$ cells of OVAS-21/om, the i.p. injection of AdCNh1 or AdGFP ($2 \times 10^8$ plaque-forming units/2 mL) was started and repeated by every 3 days until 19 days after the inoculation. In some groups, 100 mg/kg paclitaxel was given once i.p. at 3 days after inoculation. Survival and body weight of each mouse were monitored until 5 months after the inoculation, and an autopsy was done. Paclitaxel (Taxol) was kindly provided by Bristol-Myers Squibb (Tokyo, Japan).

*Scanning electron microscope.* Peritoneum was resected from abdominal walls of mice at 7 days after the i.p. inoculation of SKOV3i.p.1 cancer cells followed by the adenoviral injection. Peritoneal tissues were fixed in 1% glutaraldehyde for 12 hours followed by 1-hour fixation in 1% osmium tetroxide. After dehydration in ethanol, the specimens were rinsed in isoamyl acetate and dried by a critical point drying method. The dried specimens were mounted on copper plates and coated with osmium in an osmium plasma coater (Nippon Laser and Electronics Lab, Japan). The specimens were examined with a JSM-6000F scanning electron microscope (Jeol, Pleasonton, CA) at 1.5 kV.

*Statistical analysis.* Mann-Whitney *U* test was used to assess the statistical significance of differences in soft-agar colony-forming assay, cell motility assay, *in vitro* invasion assay, and assay for cell invasion through the peritoneal cell layer. *In vivo* tumor growth assay was assessed using Fisher's exact test. Survival curves were analyzed with Kaplan-Meier method and the difference between curves was assessed according to the log-rank test. All *P*s are two-sided and considered statistically significant at $<0.05$.

## Results

### Efficacy of *CNh1* gene transfection into the peritoneal cells

*Expression of CNh1 and three kinds of actin proteins in the transfected peritoneal cells.* Although endogenous expression of 34-kDa CNh1 protein was found in CCL14 cells infected with AdGFP or AdCNh1 (Fig. 2A) as well as noninfected CCL14 cells, exogenous CNh1 protein fused with GFP appeared additionally as a 61-kDa band in AdCNh1-infected cells (Fig. 2A). Because CNh1 is known to stabilize α-SMA, the expressions of α, β, and γ actin proteins were analyzed after *CNh1* adenoviral infection. No change of expression of any actin was observed between AdGFP-infected cells and their parental noninfected cells. Although expression of β and γ actins were not changed even by AdCNh1 infection, α-SMA expression was clearly enhanced by *CNh1* transfection (Fig. 2A and B).

*Effects of* CNh1 *gene transfection into the peritoneal cells against the destabilization of their actin filaments in the presence of conditioned medium of ovarian cancer cells.* Original peritoneal cells show well-developed actin stress fibers within their cytoplasm and well-stretched cell shape in normal culture medium. In the presence of ovarian cancer conditioned medium, we observed decreased actin stress fibers resulting in shrunken cell shape, intercellular dissociation, and cell detachment from culture plate, and this phenomenon was specifically accompanied by decreasing expressions of both CNh1 and α-SMA.[5] Therefore, we examined whether *CNh1* transfection into the peritoneal cells could stabilize actin filaments against the ovarian cancer-derived factors. As shown in Fig. 3A, AdGFP-infected cells in the presence of ovarian cancer conditioned medium showed smaller and shrunken cell shape with thin and short actin filaments at the cytosol and small spike-like filaments observed at the cellular margins, which is similar in appearance to the noninfected FK cells in the presence of ovarian cancer conditioned medium. Therefore, AdGFP infection could not recover the FK cells from ovarian cancer-derived morphologic changes. On the other hand, AdCNh1-infected cells maintained large and extended cell shape with thick and long filaments traversing a cell, just like untreated parental peritoneal cells, even in the presence of ovarian cancer conditioned medium (Fig. 3B). Localization of actin stress fiber (Fig. 3B) was identical with the expression site of *CNh1-GFP* gene products (Fig. 3C), which was

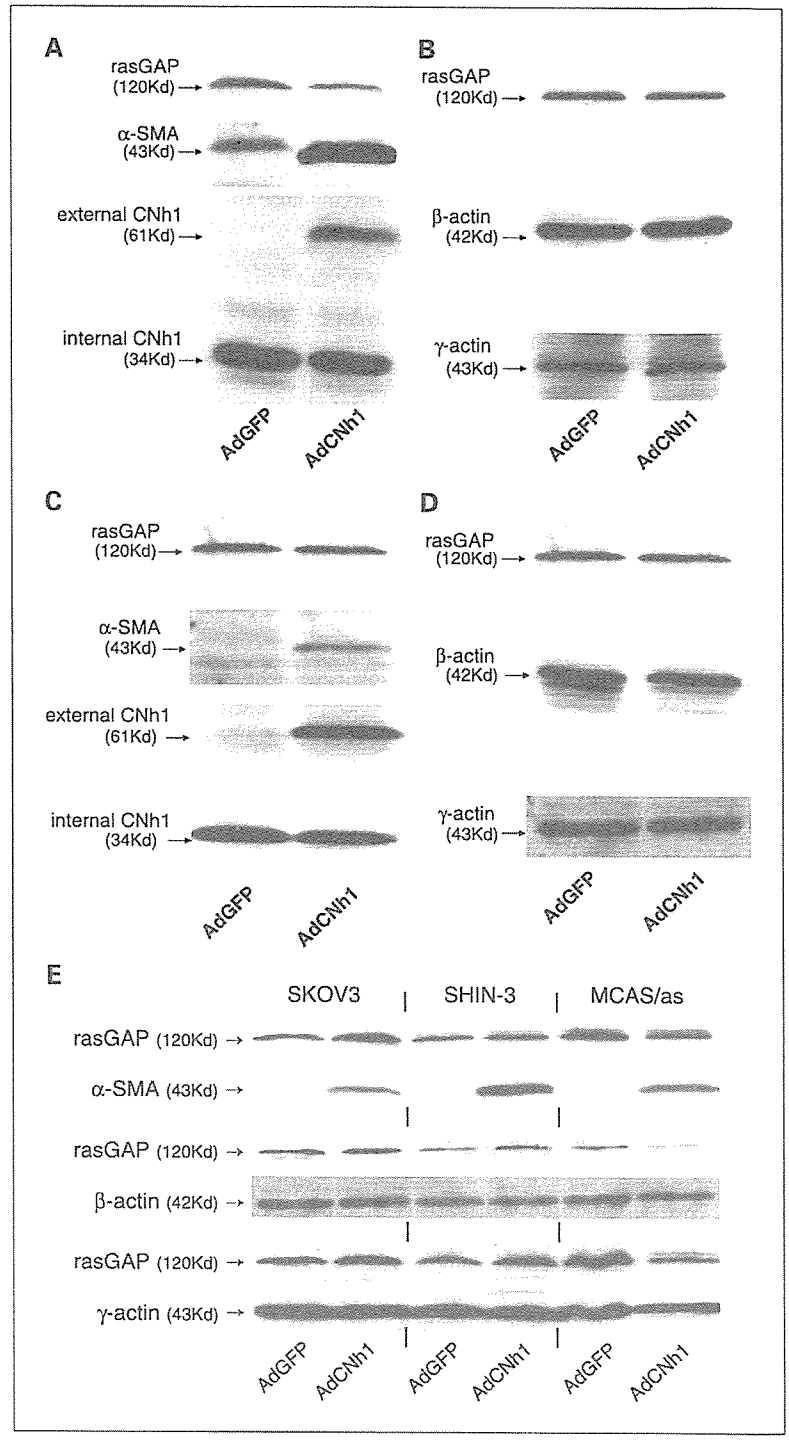


Fig. 2. Western blot analysis for the changes in expressions of CNh1 and actins after *CNh1* transfection. Expressions of CNh1 and three kinds (α-SMA, β, and γ) of actins were compared between AdCNh1 and AdGFP infections to CCL14 peritoneal cells (*A* and *B*) and the three ovarian cancer cell lines SKOV3 (*C-E*), SHIN-3 (*E*), and MCAS/as (*E*). In addition to endogenous CNh1 expression (34 kDa), external *CNh1* fused to *GFP* gene (61 kDa) was expressed in AdCNh1-infected peritoneal cells (*A*) and cancer cells (*C* and *E*). Increased α-SMA expression by *CNh1* transfection was confirmed in the peritoneal cells (*A*). Although all AdGFP-infected cancer cell lines showed an undetectable level of α-SMA expression just like their parental lines, α-SMA expression stably appeared after *CNh1* transfection in each cell line (*C* and *E*). Expressions of neither β nor γ actin was unchanged by *CNh1* transfection in both peritoneal cells (*B*) and ovarian cancer cells (*D* and *E*). Expression of rasGAP was confirmed as an internal control.

confirmed by the yellow fibers consisting of merged observation for both proteins (Fig. 3D). Therefore, the actin stress fiber development in AdCNh1-infected cells seemed to be due to the exogenously transfected *CNh1* gene.

### Efficacy of *CNh1* gene transfection into ovarian cancer cells

*Expression of CNh1 and three kinds of actin proteins in the transfected ovarian cancer cells.* Similar with the case of peritoneal cells, internal 34-kDa CNh1 protein was detected in SKOV3 ovarian cancer cells infected with AdGFP or AdCNh1 (Fig. 2C) as well as noninfected SKOV3 cells. After AdCNh1 infection, the band representing 61-kDa *CNh1-GFP* fusion protein appeared along with the induced α-SMA band (Fig. 2C). Expression of both β and γ actins was unchanged by *CNh1* transfection into SKOV3 cells (Fig. 2D and E) as well as other ovarian cancer cell lines of SHIN-3 and MCAS/as (Fig. 2E). In each cell line, AdCNh1 infection induced the high-intensity band of α-SMA compared with the "invisible" band in AdGFP-infected cells (Fig. 2E) as well as noninfected cells.

*Changes of actin filaments and cell shapes occurred in* CNh1*-transfected ovarian cancer cells.* Similar to noninfected SKOV3 cell line, AdGFP-infected SKOV3 cells showed weakly and diffusely stained actin filaments (Fig. 3E), the location of which was not identical with that of exogenously transducted GFP (Fig. 3F and G). AdCNh1 infection induced thick and long actin stress fibers and changed the cell shape into a flat and extended phenotype (Fig. 3H). The localization of the developed actin stress fibers was identical with the GFP expression sites, except the nuclear area (Fig. 3I and J), indicating that the exogenously introduced *CNh1-GFP* gene products produced the stable actin fibers. Similar results were observed in other AdCNh1-infected ovarian cancer cell lines (data not shown).

*Decreased growth property in* CNh1*-transfected ovarian cancer cells.* We confirmed that *CNh1* transfection changed neither cell growth rate nor colony-forming ability of ovarian cancer cells when growing as a monolayer culture system (data not shown). Therefore, we evaluated anchorage-independent cell growth by soft-agar colony-forming assay and found that all ovarian cancer cell lines infected with AdCNh1 formed markedly fewer colonies compared with the case of AdGFP infection (Fig. 4A).

Effects of *CNh1* transfection on tumor growth were evaluated by i.m. inoculation of parental SKOV3 cells and their subclones transfected with human *CNh1* plasmid (SKOV/CNh1) or mock vector (SKOV/mock). As shown in Fig. 4B, the *CNh1*-transfected SKOV/CNh1 cells showed significantly retarded growth, whereas the SKOV/mock cells showed almost the same growth rate as parental SKOV cells.

*Decreased invasiveness and cell locomotion in* CNh1*-transfected ovarian cancer cells.* We evaluated the effect of *CNh1* transfection on the invasiveness by an *in vitro* assay. Invasion of AdCNh1-infected SKOV-3, SHIN-3, and MCAS/as cells were all significantly decreased by 67.6%, 43.1%, and 27.6%, respectively, in contrast to AdGFP-infected controls (Fig. 5A). Because the change of cell morphology strongly correlates with cell locomotion, we examined the effects of AdCNh1 on cell motility using Matrigel-uncoated Transwell chambers. The cell motility of AdCNh1-infected each cell lines was significantly decreased by 50.5%, 44.3%, and 29.1%, respectively, in contrast to each AdGFP-infected control (Fig. 5B).

## Effects of *CNh1* gene transfection into both peritoneal cells and ovarian cancer cells

*Bifunctional inhibitory effects of* CNh1 *transfection against the invasion of cancer cells through peritoneal cell layer.* Figure 5C shows the effect of *CNh1* transfection into cancer cells and/or peritoneal cells on the cancer invasion into peritoneal cell monolayer. When either cancer cells or peritoneal cells were infected by AdCNh1, cancer cell invasion through peritoneal cell monolayer was significantly suppressed. The concomitant AdCNh1 infection into both cells produced additive and marked inhibitory effects on the cancer cell invasion.

*Effects of AdCNh1 infection on morphologic changes of peritoneal cell surface induced by ovarian cancer cells.* Scanning electron microscope showed that the i.p. inoculation of ovarian cancer cells changed the surface of murine peritoneal cells from a smooth phenotype without spikes (Fig. 6A) into an "edgy" one with numerous small spikes. This microvilli-like cell surface change was unavoidable by i.p. infection of AdGFP following cancer cell inoculation (Fig. 6B). However, i.p. injection of AdCNh1 with cancer inoculation could avoid this change,

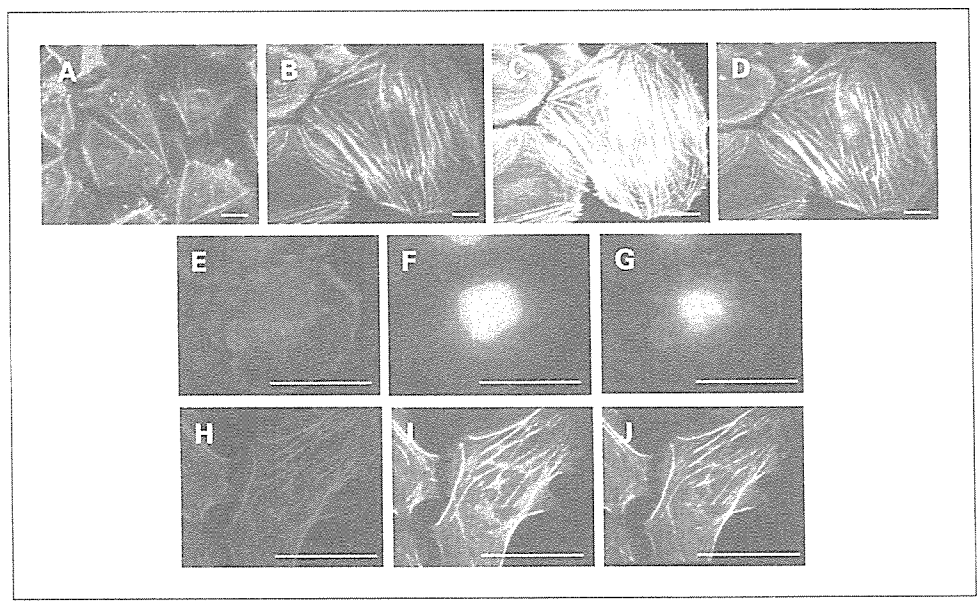


Fig. 3. F-actin staining in peritoneal cells and ovarian cancer cells and its relative localization with *CNh1-GFP* fusion gene products. *A* to *D*, human peritoneal FK cells infected with AdGFP (*A*) and AdCNh1 (*B-D*) were cultured in the presence of the conditioned medium prepared from SKOV3 ovarian cancer cells. To examine F-actin distribution by confocal laser scanning microscope, cells were fixed and stained with Alexa 568-phalloidin. Although shrunken cell shape and poor development of F-actin were observed in AdGFP-infected cells (*A*) as well as noninfected parental cells, marked development of actin stress fiber was observed in AdCNh1-infected cells with a stretched cell shape (*B*). The localization of external *CNh1-GFP* gene products observed through a FITC filter for GFP (*C*) corresponded to that of actin stress fibers, which was confirmed by the merged observation for F-actin and GFP localization (*D*). Bar, 5 μm. *E* to *J*, F-actin and GFP localization in SKOV3 ovarian cancer cells infected with AdGFP (*E-G*) or AdCNh1 (*H-J*). Although poor development of F-actin was observed mainly in perinuclear area of AdGFP-infected cells (*E*) as well as noninfected cells, the stable actin stress fibers appeared in AdCNh1-infected cells with a stretched cell shape (*H*). The localization of external *GFP* gene product (*F*) did not correspond to F-actin localization, which was confirmed by the merged observation for F-actin and GFP (*G*). On the contrary, the localization of external *CNh1-GFP* fusion gene products (*I*) obviously corresponded to F-actin localization (*J*). Bar, 5 μm.

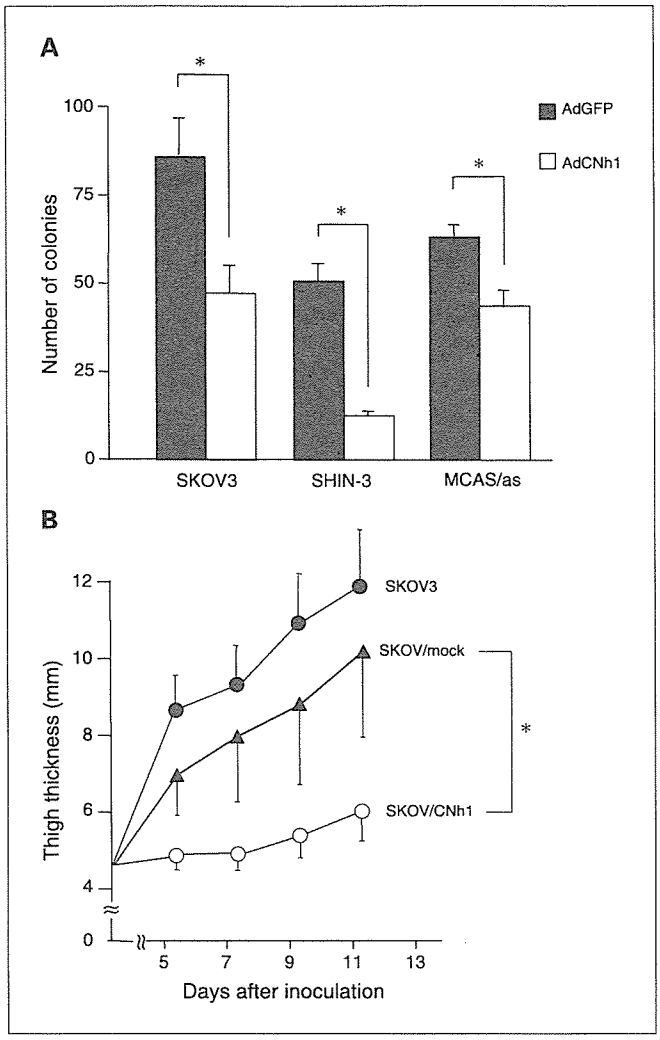


Fig. 4. Changes of growth property after *CNh1* transfection into ovarian cancer cells. *A, in vitro* cell growth was evaluated by soft-agar colony-forming assay using three ovarian cancer cell lines infected by AdGFP (*black columns*) or AdCNh1 (*white columns*). *CNh1* transfection significantly reduced anchorage-independent growth of all ovarian cancer cell lines. Columns, mean of triplicate determinations; bars, SD. *; $P < 0.05$. *B, in vivo* tumor growth was evaluated by monitoring i.m. transplanted tumor size using SKOV3 cells and their plasmid transfectants. *CNh1*-transfected SKOV/CNh1 (○) showed retarded tumor growth compared with parental SKOV3 cells (●) or control plasmid-transfected SKOV/mock (▲). Points, mean ($n = 6$ mice); bars, SD. *, $P < 0.05$, SKOV/CNh1 versus SKOV/mock in each measurement point.

resulting in a flat and smooth surface of peritoneal cells (Fig. 6C) as well as a normal surface observed in the absence of cancer cells (Fig. 6A).

In vivo *treatment for i.p. inoculated ovarian cancer cells using i.p. AdCNh1 injection with or without an anticancer drug.* Because all of the aforementioned results suggested that CNh1 suppressed ovarian cancer activity and enhanced peritoneal defense mechanisms, the potential for bifunctional therapeutic effects of AdCNh1 was investigated by treating nude mice inoculated i.p. with ovarian cancer cells. A preliminary experiment showed at least 3 days of effectiveness of i.p. injected adenovirus by monitoring the GFP expression on peritoneum (15). Therefore, AdCNh1 or AdGFP was repeatedly injected i.p. every 3 days from the next day of the inoculation with a highly i.p. disseminated cell line of OVAS-21/om, which resulted in 22 days of the median survival in untreated mice. As shown in the survival curves (Fig. 6D), the median survival of AdCNh1- or AdGFP-treated mice was 91 or 49 days, respectively, and percent increase in life span (median survival of

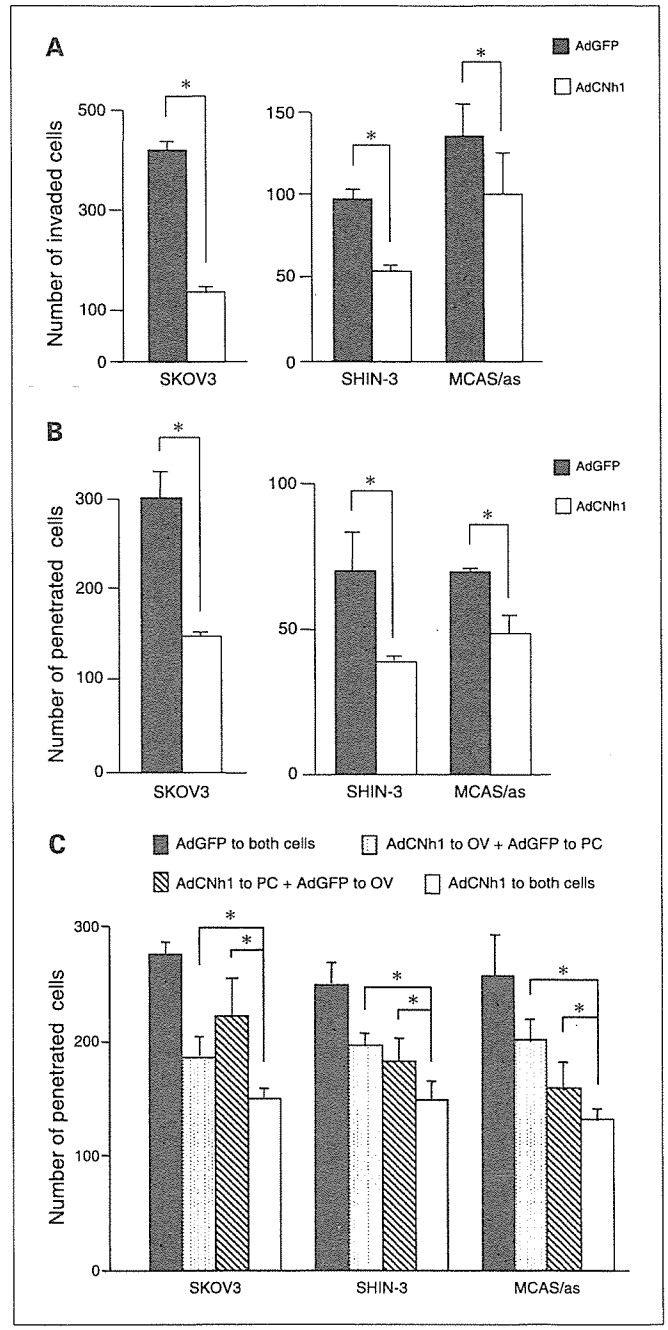


Fig. 5. Changes of invasiveness and cell motility after *CNh1* transfection into ovarian cancer cells and peritoneal cells. Cell invasiveness and motility of ovarian cancer cells were evaluated by *in vitro* invasion assay (*A*) and *in vitro* cell motility assay (*B*), respectively. AdCNh1-infected cells of all cell lines (*white columns*) showed significantly less invasive or migratory abilities compared with AdGFP-infected cells (*black columns*). Columns, mean of triplicate determinations; bars, SD. *, $P < 0.05$. *C*, effects of *CNh1* transfection for not only ovarian cancer cells but also peritoneal cells. Cancer invasion was evaluated by number of colonies derived from a cancer cell that penetrated through the monolayer of peritoneal cells. AdCNh1 infection into either ovarian cancer cells (*AdCNh1 to OV*; *dotted columns*) or peritoneal cells (*AdCNh1 to PC*; *striped columns*) resulted in significant inhibition against invasion compared with control AdGFP infection into both cells (*black columns*). Additive inhibitory effects were observed in each case when both cells were infected by AdCNh1 (*white columns*). Columns, mean of triplicate determinations; bars, SD. *, $P < 0.05$.

treated mice – median survival of untreated mice / median survival of untreated mice × 100) of AdCNh1-treated mice was 314%. We could obtain the significantly prolonged survival by AdCNh1 injection into the murine abdominal cavity ($P$ = 0.002, AdCNh1 versus AdGFP). No body weight loss was observed in either adenoviral administration.

To examine the effects of AdCNh1 combined with the administration of paclitaxel, a highly effective anticancer drug of the present mainstream for ovarian cancer treatment, 100 mg/kg paclitaxel was i.p. injected 3 days after cancer cell inoculation. As shown in Fig. 6E, although AdGFP failed to prolong the survival of paclitaxel-treated mice, additionally prolonged survival was obtained in the combined therapy by AdCNh1 and paclitaxel ($P$ = 0.04, AdCNh1 + paclitaxel versus paclitaxel alone). No aggravation was observed in toxicity by either viral administration to paclitaxel-treated mice, which transiently showed 3% body weight loss on an average.

Autopsy was done as early as possible after each mouse died from peritoneal dissemination. All of dead mice showed the distended abdomen by a massive bloody ascites and the disseminated numerous implants on the surface of i.p. organs and peritoneum (Fig. 6F). In contrast, one of six mice treated by AdCNh1 and three of five mice treated by AdCNh1 plus paclitaxel survived even 147 days after the cancer cell inoculation and showed no i.p. implants confirmed by slaughter (Fig. 6G).

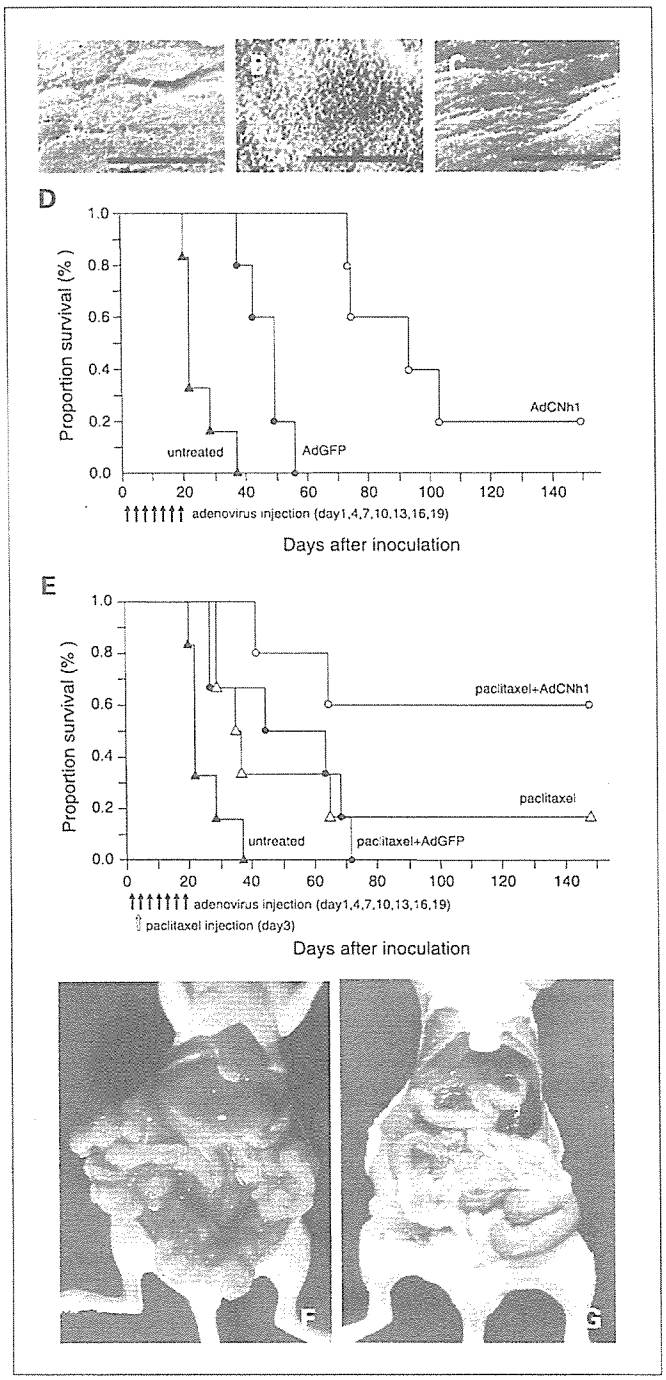


## Discussion

When intracellular globular actin is polymerized to form F-actin and the filaments of F-actin are bundled, their configurations are (*a*) big stress fiber traversing a cell, (*b*) loose and thin gelatinous filaments, and (*c*) filaments thickly lining up in microspike and lobopodium of cell periphery. It is thought that short actin filaments forming microspikes increase inversely with a decrease of long actin stress fibers, accompanying the reduction of CNh1 expression (21). We also observed that ovarian cancer-derived inhibition in CNh1 expression resulted in both decrease of actin stress fibers and formation of microspikes in peritoneal cells, both of which could be avoided by exogenous *CNh1* transfection (Figs. 3A-D and 6A-C). *CNh1*-transfected peritoneal cells did not change their diamond-shaped configuration in spite of the presence of ovarian cancer conditioned medium (Fig. 3B). These protective effects of CNh1 against ovarian cancer-derived factors enhanced the "defense" ability (i.e., resistance of peritoneal cells), which was shown by reduced cancer cell invasion through mesothelial cell layer (Fig. 5C) and by our reported data that the fragility against peritoneal dissemination of cancer observed in the *CNh1*-deficient knockout mice was rescued by the exogenous introduction of the *CNh1* gene into mesothelial cells (15).

CNh1 brought about therapeutic effects not only for host cells but also for ovarian cancer cells as well. Forced CNh1 expression in ovarian cancer cells developed actin stress fibers

**Fig. 6.** Effects of AdCNh1 injection into mice inoculated i.p. with ovarian cancer cells. *A* to *C*, morphologic changes in the cell surface of peritoneum were observed by scanning electron microscope after the i.p. inoculation of SKOV3i.p.1 cancer cells. The surface of peritoneal cells changed from the ordinary flat and smooth cell surface (*A*) into a "fluffy" phenotype accompanied by many microspikes, and this change was not avoided by AdGFP (*B*). However, AdCNh1 could maintain almost normal cell surface against the ovarian cancer-derived influence (*C*). Bar, 10 μm. *D* and *E*, therapeutic effects of AdCNh1 i.p. injection combined with or without paclitaxel were evaluated by the survival of treated mice. AdCNh1 or AdGFP was repeatedly injected i.p. after the i.p. inoculation of OVAS-21/om cancer cells (*D*). Significantly prolonged survival was observed in AdCNh1-treated mice (○) compared with AdGFP-treated mice (●; $P$ = 0.002). Paclitaxel was i.p. injected 3 days after tumor inoculation to examine the effects of AdCNh1 combined with anticancer drug (*E*). Additionally prolonged survival was obtained in the combined therapy by AdCNh1 and paclitaxel (○) compared with the therapy by paclitaxel alone (△; $P$ = 0.04). *F* and *G*, i.p. appearances after the adenoviral treatment were shown by representative mice. An AdGFP-treated mouse, died 49 days after the inoculation, showed peritonitis carcinomatosa with massive ascites accompanied by numerous disseminated implants on the surface of i.p. organs and peritoneum (*F*). In contrast, an AdCNh1-treated mouse, which survived even 147 days after the inoculation, showed neither ascites nor i.p. implants (*G*). As for the side effects of AdCNh1 treatment, neither body weight loss nor intra-abdominal adhesion was observed.

accompanying α-SMA induction (Figs. 2C-E and 3H-J), which resulted in retardation of growth and invasiveness (Figs. 4 and 5A). As for growth-inhibitory effects mediated by CNh1, *in vitro* anchorage-independent cell growth (Fig. 4A) and *in vivo* tumor growth (Fig. 4B) were both suppressed, although *in vitro* growth was not inhibited when cells were cultured as monolayers. As for CNh1-inhibitory effect on invasiveness, cell motility was significantly retarded (Fig. 5B). These results would seem reasonable, considering that CNh1-induced stabilization of actin stress fibers inhibits both three-dimensional cell growth and cell locomotion, for which dynamic state of actin filaments is thought to be essential. *In vivo* efficacy of CNh1 specific to ovarian cancer cells was confirmed by *CNh1*-plasmid transfectants of SKOV3i.p.1, which survived much longer than the mock transfectant (data not shown).

Cotransfection of *CNh1* into both peritoneal cells and ovarian cancer cells resulted in additive inhibition of cancer cell invasion through peritoneal cell layer compared with the inhibitory effect of *CNh1* transfection into either cell population alone (Fig. 5C). *In vivo* therapeutic effects of CNh1 were confirmed by the i.p. administration of *CNh1* adenoviral vector into nude mice bearing i.p. inoculated ovarian cancer cells (Fig. 6D). We observed that ovarian cancer cells seemed to easily invade through the peritoneal layer, which consisted of retracted and dissociated mesothelial cells with poor actin stress fiber development. This may be due to the down-regulation of CNh1 and α-SMA induced by ovarian cancer cell–derived secretory factor(s), including platelet-derived growth factor.[5] Effects of AdCNh1 used to infect both mesothelial cells and ovarian cancer cells are summarized as follows: (*a*) peritoneal cells with developed actin stress fiber had a greater ability to act as a barrier against cancer cells, avoiding ovarian cancer-induced suppression of CNh1 and α-SMA expression, and (*b*) ovarian cancer cells impaired their growth and invasion properties by induced actin stress fibers. As such, adenovirus-mediated *CNh1* gene therapy against peritoneal dissemination of ovarian cancer may be considered as a potentially novel therapeutic intervention, whereby one and the same gene has two distinctive major effects: one is to control the cancer cells and the other is to bolster a host defense (anti-invasive) mechanism.

Considering clinical application of this therapy, preventive administration of AdCNh1 just after the optimal surgery would be desirable for effective inhibition of peritoneal dissemination. At least, it seems to be difficult for this therapy to eradicate the established and large peritoneal implants. Because AdCNh1 could successfully enhance the therapeutic effect of paclitaxel without increase in side effects (Fig. 6E and G), *CNh1* gene therapy may be safely repeatable and hence potentially to improve patient prognosis especially when used in combination with conventional postoperative chemotherapy. Gene therapy using i.v. given adenovirus can be compromised in situations where the injected adenovirus is easily and rapidly washed out from the tumor site by bloodstream (22). However, adenoviral gene therapy using i.p. injection has an advantage in that the adenovirus can stay at the site of target cells (cancer cells and peritoneal cells), owing to the closed space of the "abdominal cavity." With respect to the problem of decreasing efficacy in repeating adenovirus gene therapy by appearance of human antibody against adenovirus, we would like to expect developing more suitable i.p. vector system or finding a nontoxic small molecule that can effectively enhance CNh1 expression after i.p. administration.

## Acknowledgments

We thank T. Sonoda, M. Mitsumoto, Y. Kawano, K. Fukushima, S. Miyamoto, T. Kaku, E. Hori, and S. Adachi for technical assistance and critical comments on our study, Drs. S. Minami, Y. Yoshikawa, and M. Noguchi for providing us with ovarian cancer cell lines (MCAS/as and OVAS-21/om), Dr. I.J. Fidler for the SKOV3i.p.1 cell line, and Bristol-Myers Squibb for providing paclitaxel.

## References

1. Ramaswamy S, Ross KN, Lander ES, Golub TR. A molecular signature of metastasis in primary solid tumors. Nat Genet 2003;33:49–54.
2. Takahashi K, Hiwada K, Kokubu T. Isolation and characterization of a 34,000-dalton calmodulin- and F-actin-binding protein from chicken gizzard smooth muscle. Biochem Biophys Res Commun 1986;141:20–6.
3. Strasser P, Gimona M, Moessler H, Herzog M, Small JV. Mammalian calponin. Identification and expression of genetic variants. FEBS Lett 1993;330:13–8.
4. Applegate D, Feng W, Green RS, Taubman MB. Cloning and expression of a novel acidic calponin isoform from rat aortic vascular smooth muscle. J Biol Chem 1994;269:10683–90.
5. Trabelsi-Terzidis H, Fattoum A, Represa A, Dessi F, Ben-Ari Y, der Terrossian E. Expression of an acidic isoform of calponin in rat brain: Western blots on one- or two-dimensional gels and immunolocalization in cultured cells. Biochem J 1995;306:211–5.
6. Childs TJ, Watson MH, Novy RE, Lin JJ, Mak AS. Calponin and tropomyosin interactions. Biochem Biophys Acta 1992;1121:41–6.
7. Graceffa P. Evidence for interaction between smooth muscle tropomyosin and caldesmon. FEBS Lett 1987;218:139–42.
8. Winder SJ, Walsh MP. Calponin: thin filament-linked regulation of smooth muscle contraction. Cell Signal 1993;5:677–86.
9. Shirinsky VP, Biryukov KG, Hettasch JM, Sellers JR. Inhibition of the relative movement of actin and myosin by caldesmon and calponin. J Biol Chem 1992;267:15886–92.
10. Noda S, Ito M, Watanabe S, Takahashi K, Maruyama K. Conformational changes of actin induced by calponin. Biochem Biophys Res Commun 1992;185:481–7.
11. Kobayashi H, Tsuruchi N, Sugihara K, et al. Expression of α-smooth muscle actin in benign or malignant ovarian tumors. Gynecol Oncol 1993;48:308–13.
12. Okamoto-Inoue M, Nakayama J, Hori Y, Taniguchi S. Human malignant melanoma cells release a factor that inhibits the expression of smooth muscle α-actin. J Dermatol Sci 2000;23:170–7.
13. Sobue K, Sellers JR. Caldesmon, a novel regulatory protein in smooth muscle and nonmuscle actomyosin systems. J Biol Chem 1991;266:12115–8.
14. Taniguchi S, Takeoka M, Ehara T, et al. Structural fragility of blood vessels and peritoneum in calponin h1-deficient mice, resulting in an increase in hematogenous metastasis and peritoneal dissemination of malignant tumor cells. Cancer Res 2001;61:7627–34.
15. Hashimoto S, Takeoka M, Taniguchi S. Suppression of peritoneal dissemination through protecting mesothelial cells from retraction by cancer cells. Int J Cancer 2003;107:557–63.
16. Horiuchi A, Nikaido T, Taniguchi S, Fujii S. Possible role of calponin h1 as a tumor suppressor in human uterine leiomyosarcoma. J Natl Cancer Inst 1999;91:790–6.
17. Takeoka M, Ehara T, Sagara J, Hashimoto S, Taniguchi S. Calponin h1 induced a flattened morphology and suppressed the growth of human fibrosarcoma HT1080 cells. Eur J Cancer 2002;38:436–42.
18. Xu L, Xie K, Mukaida N, Matsushima K, Fidler IJ. Hypoxia-induced elevation in interleukin-8 expression by human ovarian carcinoma cells. Cancer Res 1999;59:5822–9.
19. Ueoka Y, Kato K, Wake N. Hepatocyte growth factor modulates motility and invasiveness of ovarian carcinomas via ras mediated pathway. Mol Cell Endocrinol 2003;202:81–8.
20. Kobayashi H, Moniwa N, Gotoh J, Sugimura M, Terao T. Role of activated protein C in facilitating basement membrane invasion by tumor cells. Cancer Res 1994;54:261–7.
21. Gimona M, Kaverina I, Resch GP, Vignal E, Burgstaller G. Calponin repeats regulate actin filament stability and formation of podosomes in smooth muscle cells. Mol Biol Cell 2003;14:2482–91.
22. Kass-Eisler A, Falck-Pedersen E, Elfenbein DH, Alvira M, Buttrick PM, Leinwand LA. The impact of developmental stage, route of administration and the immune system on adenovirus-mediated gene transfer. Gene Ther 1994;1:395–402.

JCOG
Japan Clinical Oncology Group

**Japan Clinical Oncology Group(日本臨床腫瘍研究グループ)**
**婦人科腫瘍グループ**

厚生労働省　厚生労働科学研究費補助金「第 3 次対がん総合戦略研究事業」(平成 16 年度～)
「進行卵巣がんの集学的治療に関する研究」班
厚生労働省　がん研究助成金
「婦人科悪性腫瘍に対する新たな治療法の開発に関する研究」班
厚生労働省　がん研究助成金指定研究(17 指-1)
「高感受性悪性腫瘍に対する標準的治療確立のための多施設共同研究」班
厚生労働省　がん研究助成金指定研究(17 指-5)
「多施設共同研究の質の向上のための研究体制確立に関する研究」班

# JCOG0602

## OV-NACTC-P3
## III 期/IV 期卵巣癌、卵管癌、腹膜癌に対する 手術先行治療 vs. 化学療法先行治療 のランダム化比較試験実施計画書 Ver.1.0

研究代表者：吉川裕之(筑波大学臨床医学系産科婦人科)
〒305-8575 茨城県つくば市天王台 1-1-1
TEL：029-853-3049
FAX：029-853-3072
E-mail：hyoshi@md.tsukuba.ac.jp

研究事務局：恩田貴志(国立がんセンター中央病院婦人科)
〒104-0045 東京都中央区築地 5-1-1
TEL：03-3542-2511
FAX：03-3542-3815
E-mail：taonda@ncc.go.jp

2005 年 2 月 26 日　JCOG 運営委員会プロトコールコンセプト承認(PC411)
2006 年 5 月 15 日　JCOG プロトコール審査委員会一次審査提出
2006 年 8 月 15 日　JCOG プロトコール審査委員会二次審査提出
2006 年 10 月 18 日　JCOG プロトコール審査委員会承認

# 0. 概要

## 0.1. シェーマ

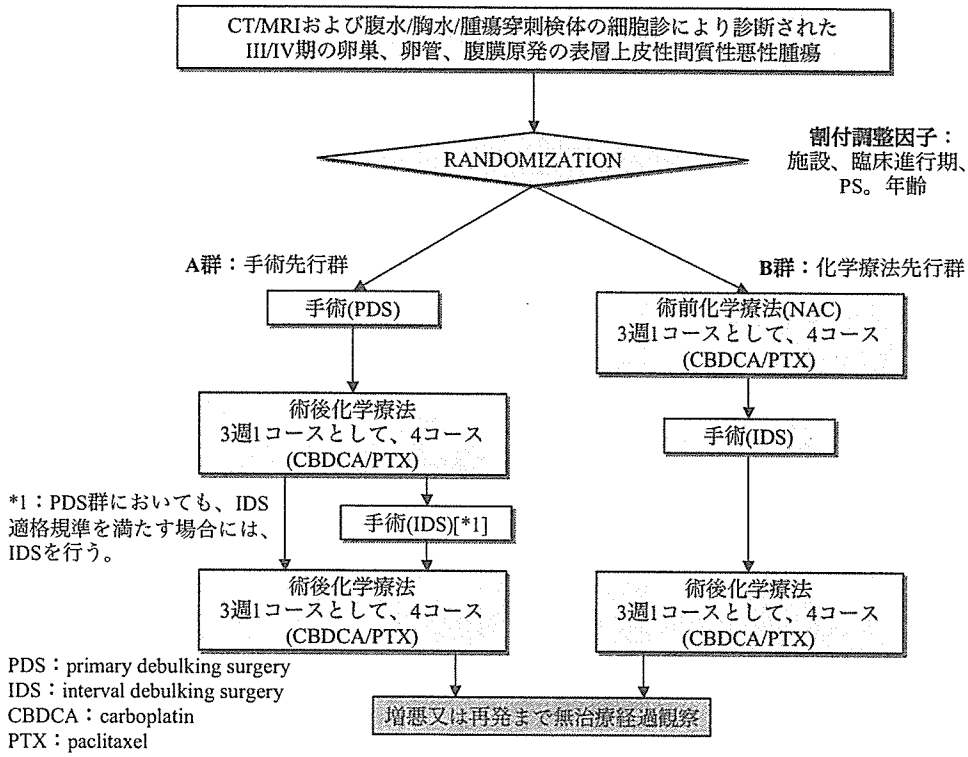


## 0.2. 目的

III、IV 期の卵巣癌、卵管癌、腹膜癌に対して、手術の前後に 4 コースずつ計 8 コースのパクリタキセル＋カルボプラチン併用化学療法を行う「化学療法先行治療」が、現在の標準治療である、手術後に計 8 コースのパクリタキセル＋カルボプラチン併用化学療法を行う「手術先行治療」よりも有用であるかどうかをランダム化比較試験にて検証する。

Primary endpoint：全生存期間

Secondary endpoints：完全腫瘍消失割合、無増悪生存期間、奏効割合(B 群のみ)、有害事象、手術侵襲指標(開腹手術回数、総開腹手術時間、出血量、総輸血量、総血漿製剤使用量)

## 0.3. 対象

以下の全てを満たす患者を対象とする。

1) 卵巣、卵管、腹膜いずれかの原発の悪性腫瘍と臨床的に診断される。
2) 細胞診所見により、卵巣の表層上皮性間質性の悪性腫瘍に相当する組織型が推定される。
3) 臨床進行期 III 期または IV 期と診断し得る。
4) 初回腫瘍縮小手術(PDS)の対象となりうる。
5) CA125>200 U/ml かつ CEA<20 ng/ml
6) 年齢：20 才以上 75 才以下
7) PS(ECOG)：0-3
8) 測定可能病変の有無は問わない。
9) 当該疾患に対して手術の既往が無く、他のがん種に対する治療も含めて化学療法、放射線照射、何れの既往もないこと。
10) 諸臓器機能が保たれている。(登録前 14 日以内の最新の検査による。)
11) 試験参加について、本人より文書による同意(インフォームド・コンセント)が得られた患者。